Polo kinase Cdc5 associates with centromeres to facilitate the removal of centromeric cohesin during mitosis

Prashant K. Mishra[a], Sultan Ciftci-Yilmaz[a,†,‡], David Reynolds[b,†], Wei-Chun Au[a], Lars Boeckmann[a], Lauren E. Dittman[a], Ziad Jowhar[a], Tejaswini Pachpor[a], Elaine Yeh[c], Richard E. Baker[d], M. Andrew Hoyt[b], Damien D'Amours[e], Kerry Bloom[c], and Munira A. Basrai[a,*]

[a]Genetics Branch, National Cancer Institute, National Institutes of Health, Bethesda, MD 20892; [b]Department of Biology, Johns Hopkins University, Baltimore, MD 21218; [c]Department of Biology, University of North Carolina, Chapel Hill, NC 27599; [d]Department of Microbiology and Physiological Systems, University of Massachusetts Medical School, Worcester, MA 01655; [e]Institute for Research in Immunology and Cancer and Département de Pathologie et Biologie Cellulaire, Université de Montréal, Montreal, QC H3C 3J7, Canada

ABSTRACT **Sister chromatid cohesion is essential for tension-sensing mechanisms that monitor bipolar attachment of replicated chromatids in metaphase. Cohesion is mediated by the association of cohesins along the length of sister chromatid arms. In contrast, centromeric cohesin generates intrastrand cohesion and sister centromeres, while highly cohesin enriched, are separated by >800 nm at metaphase in yeast. Removal of cohesin is necessary for sister chromatid separation during anaphase, and this is regulated by evolutionarily conserved polo-like kinase (Cdc5 in yeast, Plk1 in humans). Here we address how high levels of cohesins at centromeric chromatin are removed. Cdc5 associates with centromeric chromatin and cohesin-associated regions. Maximum enrichment of Cdc5 in centromeric chromatin occurs during the metaphase-to-anaphase transition and coincides with the removal of chromosome-associated cohesin. Cdc5 interacts with cohesin in vivo, and cohesin is required for association of Cdc5 at centromeric chromatin. Cohesin removal from centromeric chromatin requires Cdc5 but removal at distal chromosomal arm sites does not. Our results define a novel role for Cdc5 in regulating removal of centromeric cohesins and faithful chromosome segregation.**

Monitoring Editor
Orna Cohen-Fix
National Institutes of Health

Received: Jan 4, 2016
Revised: Apr 27, 2016
Accepted: May 19, 2016

INTRODUCTION

Accurate chromosome segregation is important for the maintenance of genome stability during growth and proliferation of organisms (Lengauer *et al.*, 1998; Maddox *et al.*, 2012). Errors in chromosome segregation result in aneuploidy, which has been linked with several human diseases, such as developmental disorders and many cancers (Santaguida and Amon, 2015; Singh and Gerton, 2015). The kinetochore, composed of centromeric DNA (*CEN*) and associated proteins, is an essential component of the chromosomal segregation machinery (Burrack and Berman, 2012; Choy *et al.*, 2012; Maddox *et al.*, 2012). The assembly of kinetochore proteins at budding yeast *CEN* (core centromere composed of ~125 base pairs of defined DNA sequences) results in a highly ordered, unique, and topologically distinct chromatin structure in the chromosomes (Clarke and Carbon, 1980; Bloom and Carbon, 1982; Bloom *et al.*, 1984; Saunders *et al.*, 1990), the structural integrity of which is required for accurate chromosome segregation (Newlon, 1988; Verdaasdonk and Bloom, 2011; Haase *et al.*, 2013; Mishra *et al.*, 2013; Mishra *et al.*, 2015). Budding yeast centromeric chromatin

This article was published online ahead of print in MBoC in Press (http://www.molbiolcell.org/cgi/doi/10.1091/mbc.E16-01-0004) on May 25, 2016.

†These authors contributed equally to this work.

‡Present address: Department of Medical Genetics, Faculty of Medicine, Turgut Ozal University, 06010 Ankara, Turkey.

*Address correspondence to: Munira A. Basrai (basraim@nih.gov).

Abbreviations used: *CAR*, cohesin-associated region; *CEN*, centromere; ChIP, chromatin immunoprecipitation; C-loop, centromere loop; GFP, green fluorescent protein; qPCR, quantitative PCR; RC, reporter chromosome; RFP, red fluorescent protein.

(*CEN* and pericentromeric DNA that extends ~30–50 kb around the *CEN*) exhibits a cruciform structure referred to as centromere loop (C-loop), which is analogous to that proposed in the looping model for vertebrate centromeres (Yeh *et al.*, 2008; Verdaasdonk *et al.*, 2012). The intramolecular linkages in the C-loop and the intermolecular linkages along the length of the chromosomes promote the biorientation of kinetochores and sister chromatids toward opposite spindle pole bodies for faithful chromosome segregation.

Cohesion along the length of the chromosomes is facilitated by chromosomal association of cohesins (Hornig and Uhlmann, 2004; Gerton, 2007; Brooker and Berkowitz, 2014). The cohesin complex is composed of four subunits: Scc1/Mcd1, Scc3, Smc1, and Smc3 (Hartman *et al.*, 2000; Laloraya *et al.*, 2000; Nasmyth, 2002; Glynn *et al.*, 2004; Weber *et al.*, 2004; Gerton, 2005; Bose and Gerton, 2010; Rossio *et al.*, 2010; Marston, 2014; Roccuzzo *et al.*, 2015). An enrichment of cohesins is seen at cohesin-associated regions (*CAR*s) and at centromeric chromatin (Blat and Kleckner, 1999; Megee *et al.*, 1999; Tanaka *et al.*, 1999). Removal of cohesins from chromosomes facilitates separation of sister chromatids at anaphase and cell cycle progression (Hartman *et al.*, 2000; Marston, 2014; Guacci *et al.*, 2015). Evolutionarily conserved Cdc5 has been shown to regulate several aspects of mitosis (Zitouni *et al.*, 2014; Archambault *et al.*, 2015), including sister chromatid separation, by phosphorylating Scc1/Mcd1 (Alexandru *et al.*, 2001) to promote its proteolytic cleavage by separase (Uhlmann *et al.*, 2000). Mutation of phosphorylatable serines to alanines in Scc1/Mcd1 or depletion of Cdc5 results in anaphase delay (Alexandru *et al.*, 2001; Hornig and Uhlmann, 2004). It has been proposed that preferential phosphorylation of chromatin-bound Scc1/Mcd1 by Cdc5 accelerates its cleavage compared with soluble cohesin (Hornig and Uhlmann, 2004); however, not all Scc1/Mcd1 is cleaved by separase in anaphase (Uhlmann *et al.*, 1999).

Here we report that Cdc5 associates with centromeric chromatin and *CAR*s in a cell cycle–dependent manner. Enrichment of Cdc5 in mitosis overlaps with the timing of removal of cohesin from chromosomes. Cohesin proteins interact with Cdc5 in vivo and are required for the enrichment of Cdc5 at centromeric chromatin during mitosis. We demonstrate the persistence of centromeric cohesin in anaphase cells of a *cdc5* mutant. Our results show that Cdc5 associates with centromeric chromatin to regulate the removal of cohesin from this region and promote faithful chromosome segregation.

RESULTS

Cdc5 associates with centromeric chromatin in a cell cycle–dependent manner

To determine whether Cdc5 associates with centromeric chromatin, we performed chromatin immunoprecipitation (ChIP) experiments using a wild-type strain carrying hemagglutinin (HA)-tagged Cdc5 expressed from its own promoter. ChIP–quantitative PCR (qPCR) showed that Cdc5 associates with core *CEN* (*CEN1* and *CEN5*) in logarithmically growing cells (Figure 1A). No significant enrichment of Cdc5 was observed at the negative control region *6K120* (Rossio *et al.*, 2010) or in an untagged wild-type strain (Figure 1A). We next examined Cdc5 enrichment in chromatin regions flanking *CEN*. ChIP-qPCR showed that Cdc5 is strongly enriched at the central core region of *CEN3* and flanking chromatin (Figure 1B). No significant enrichment was detected in an untagged wild-type strain used as a control (Figure 1, A and B).

To examine whether association of Cdc5 with *CEN* varies during the cell cycle, we performed ChIP experiments using a wild-type strain arrested in the G1 (α-factor treatment), S (hydroxyurea treatment), or M (nocodazole treatment) phases of the cell cycle. The cell cycle arrest was confirmed by fluorescence-activated cell sorting (FACS) assay (Supplemental Figure S1). Western blot analysis revealed a cell cycle–dependent expression pattern of Cdc5, with maximum protein levels observed in M-phase cells, only low levels detected in S-phase cells, and no detectable expression in G1 cells (Figure 1C), as previously observed (Hardy and Pautz, 1996; Charles *et al.*, 1998). The *CEN* enrichment of Cdc5 was significantly higher in mitotic (M) cells (Figure 1D). No significant enrichment of Cdc5 at *CEN* was detected in G1- and S-phase cells; the ChIP signals in G1- and S-phase cells were largely similar to those detected at a negative control region, *6K120* (Figure 1D). Control experiments performed with an untagged wild-type strain showed no significant enrichment of Cdc5 at either *CEN* or negative control region *6K120* (Supplemental Figure S2).

Next we examined the *CEN* association of Cdc5 during cell cycle progression using wild-type cells arrested in G1 phase by α-factor treatment and at various times after release from G1 arrest (Figure 2A). On the basis of cell and nuclear morphology, we categorized cells as G1, S, metaphase (ME), anaphase (A), and telophase (T) following procedures described previously (Calvert and Lannigan, 2010). In agreement with previous results (Figure 1B), Western blot analysis revealed cell cycle–regulated expression of Cdc5, with increased levels observed in metaphase and anaphase cells (Figure 2B). ChIP results showed that *CEN* association of Cdc5 is low in cells soon after release from α-factor arrest (40 min), increasing as cells enter mitosis (60 min), maximum in anaphase (80 min), and decreasing as cells exit mitosis (100–120 min; Figure 2, A and C). We did not detect Cdc5 enrichment at a negative control region, *6K120* (Figure 2C bottom). On the basis of these results, we conclude that *CEN* association of Cdc5 is cell cycle dependent, with maximum enrichment in mitosis (metaphase and anaphase).

Because a previous study showed enrichment of Cdc5 at *CAR*s (Rossio *et al.*, 2010), we investigated whether Cdc5 localization at *CAR*s is cell cycle dependent. We examined three *CAR*s on chromosome III (Figure 3A, green triangles), and two non-*CAR*s (Figure 3A, black vertical lines) previously reported to either associate or fail to associate with cohesin components, respectively (Eckert *et al.*, 2007; Ng *et al.*, 2009). The *CAR*s are 114 (*CEN3*), 134 (peri-*CEN*, 20 kb from *CEN3*), and 261 (chromosome arm, 147 kb from *CEN3*), and non-*CAR*s are 125 (peri-*CEN*, 11 kb from *CEN3*) and 266 (chromosome arm, 152 kb from *CEN3*; Figure 3A). Experiments performed with an untagged wild-type strain showed no significant enrichment of Cdc5 at any of the regions tested (Figure 3B). In logarithmically growing cells, Cdc5 associates specifically with *CAR*s (Figure 3B). Cdc5 enrichment at *CAR*s was significantly higher in mitotic cells (M) than in S-phase cells and was barely detectable in G1 (Figure 3C). The increased levels of Cdc5 at *CAR*s in mitosis were verified by assaying cells synchronized in G1 and released into pheromone-free medium. Consistent with the increased enrichment of Cdc5 at peri-*CEN* and arm *CAR*s (134 and 261, respectively) in nocodazole-treated cells (Figure 3C), we observed higher levels of Cdc5 at these regions in cells undergoing mitosis (60–100 min postrelease; Figure 4). Taken together, these results show that Cdc5 enrichment at *CEN* and *CAR*s is cell cycle dependent, with maximum enrichment during mitosis.

Induced expression of Cdc5 in G1 does not result in its recruitment to centromeric chromatin and *CAR*s

The mitotic enrichment of Cdc5 at *CEN* and *CAR* sites correlates with the protein expression levels of Cdc5, and no significant enrichment of Cdc5 was observed at these sites in G1, when protein expression of Cdc5 was not detected (Figure 1, C and D). Therefore

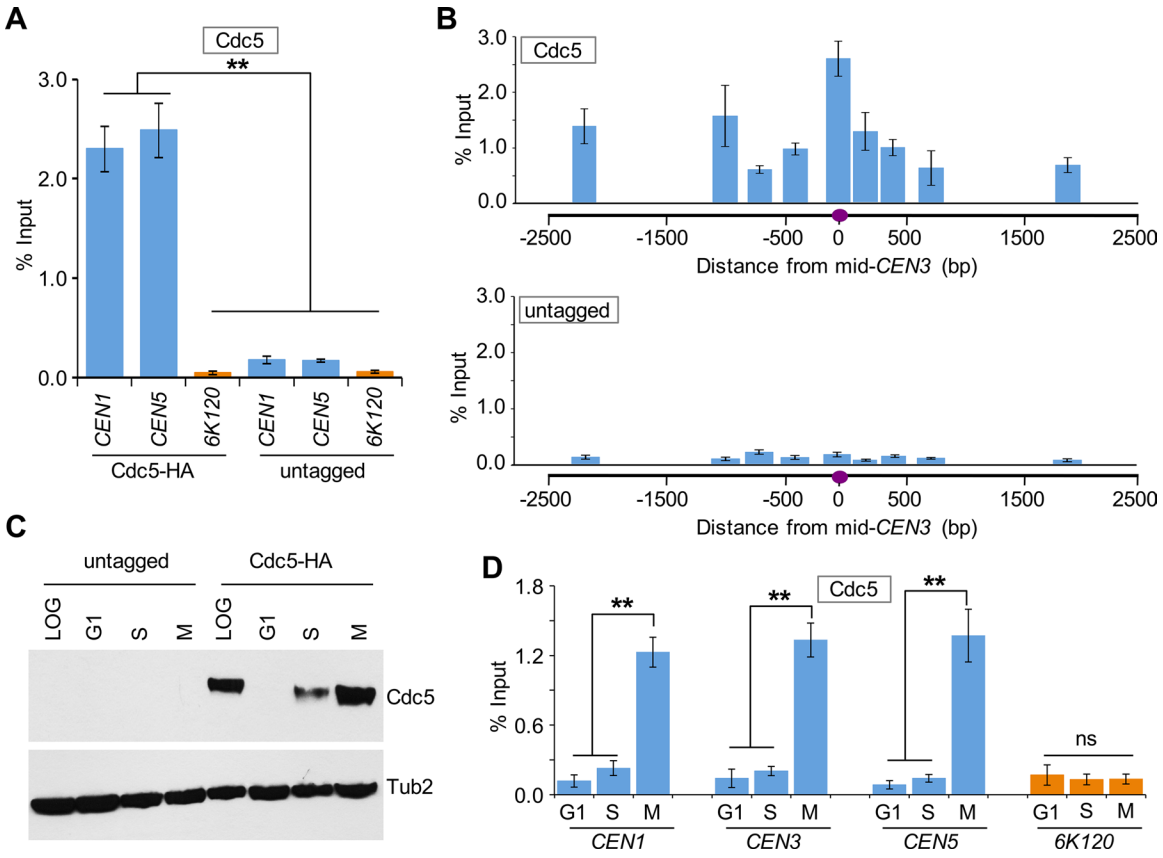

FIGURE 1: Cdc5 associates with centromeric chromatin in a cell cycle–dependent manner. (A) Cdc5 associates with core *CEN* DNA. ChIP was performed for Cdc5 using a wild-type strain containing Cdc5-HA (YMB9264) and an untagged control strain (YMB9263). Strains were grown to logarithmic phase at 30°C. ChIP was performed using α-HA antibodies. Enrichment of Cdc5 to *CEN1* and *CEN5* as determined by qPCR is shown as percentage input. The negative control region *6K120* was used as a background control. Average from three biological replicates ± SE. $^{**}p < 0.01$, Student's *t* test. (B) Cdc5 is enriched at the *CEN* and peri-*CEN* chromatin. ChIP was performed as in A. Average from three biological replicates ± SE. (C) Western blotting showing the protein expression levels of Cdc5-HA in wild-type strain containing Cdc5-HA (YMB9264) and untagged control (YMB9263). Strains were in logarithmic phase of growth (LOG) or arrested in G1-phase (α-factor), S-phase (hydroxyurea), or M-phase (nocodazole) stages of the cell cycle. Antibodies used in Western blotting were α-HA (Cdc5) and α-Tub2 (loading control). (D) Association of Cdc5 with *CEN* DNA increases in mitotic cells. ChIP-qPCR shows the levels of *CEN*-associated Cdc5 in a wild-type strain containing Cdc5-HA (YMB9264) and untagged control (YMB9263) grown to logarithmic phase at 30°C or arrested at various stages of the cell cycle as in C. Enrichment at *CEN* (*CEN1*, *CEN3,* and *CEN5*) and a negative control region *6K120* was determined by qPCR and is shown as percentage input. Average from three biological replicates ± SE. $^{**}p < 0.01$; ns, not statistically significant, Student's *t* test.

we sought to determine whether recruitment of Cdc5 at *CEN* and *CAR* sites is regulated by the cell cycle or is an outcome of its cell cycle–dependent expression pattern. We constructed a strain expressing HA-tagged Cdc5 from a galactose-inducible promoter (*GAL1-3HA-CDC5*) and performed ChIP experiments using cells growing logarithmically and cells arrested in G1 with α-factor treatment. The galactose-induced expression of Cdc5 in logarithmically growing and G1 cells was determined by Western blotting (Figure 5A). FACS analysis confirmed the synchronization of cells in G1 (Figure 5B). ChIP-qPCR revealed significant enrichment of Cdc5 at *CEN3* and *CAR*s (134, 261) in logarithmically growing cells, but no significant enrichment of Cdc5 was detected at these regions in G1 cells (Figure 5C). The ChIP signals in G1 cells were largely similar to those detected at the negative control region *6K120* or at *CEN3, CAR*s, and *6K120* region in an untagged wild-type strain (Figure 5C). On the basis of these results, we conclude that the enrichment of Cdc5 at *CEN* and *CAR*s is cell cycle regulated.

Cohesin proteins interact with Cdc5 and regulate the mitotic enrichment of Cdc5 at centromeric chromatin and *CAR*s

The association of Cdc5 at *CEN* and *CAR*s (Figures 1–4) coincides with the high levels of cohesins shown to associate at these regions (Megee *et al.*, 1999; Laloraya *et al.*, 2000; Glynn *et al.*, 2004; Weber *et al.*, 2004; Eckert *et al.*, 2007); hence we asked whether cohesin interacts with Cdc5 in vivo and investigated its role in Cdc5 centromeric association. In budding yeast, the cohesin complex is composed of four subunits: Scc1/Mcd1, Scc3, Smc1, and Smc3 (Nasmyth, 2002). We constructed strains expressing Cdc5 and TAP-tagged Mcd1 or Cdc5 and green fluorescent protein (GFP)–tagged Smc3 from their endogenous promoters. Immunoprecipitation experiments showed in vivo interaction of Cdc5 with Mcd1 and Smc3 (Figure 6). No interaction was observed in control experiments using a strain with untagged Mcd1 or Smc3 (Figure 6).

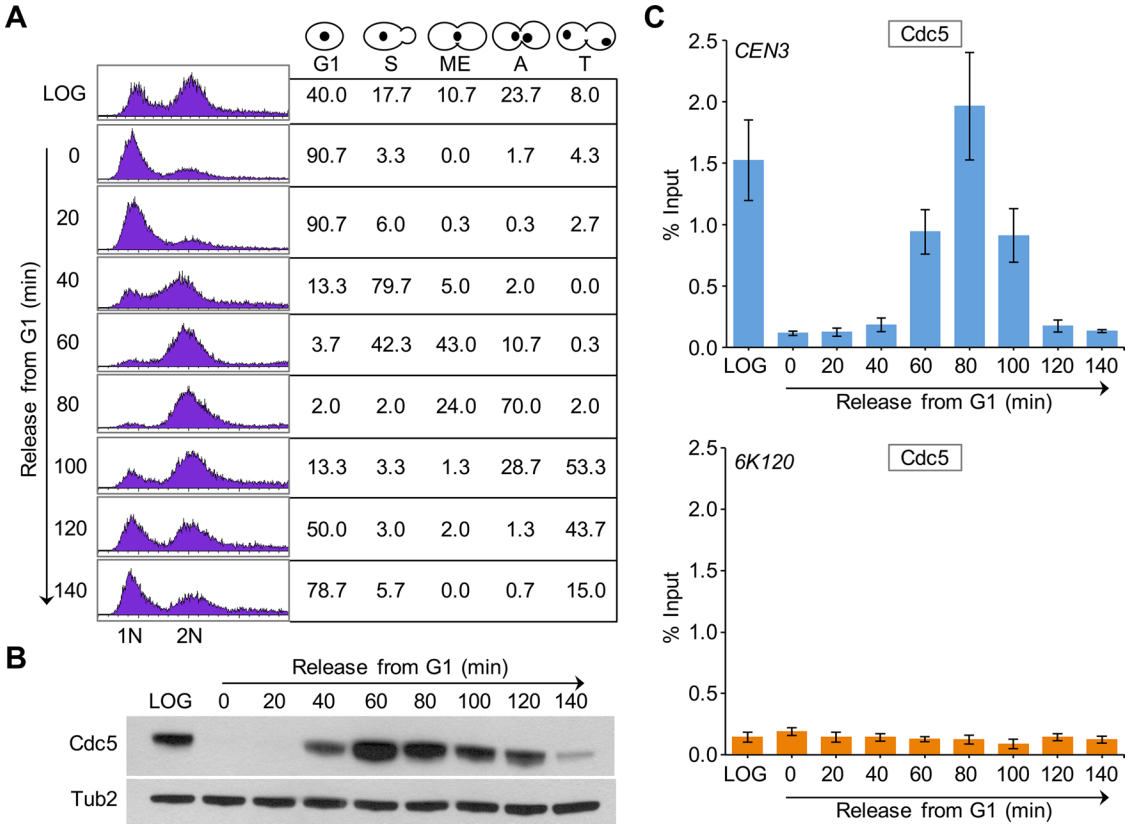

FIGURE 2: *CEN* association of Cdc5 is cell cycle regulated, with maximum enrichment in cells undergoing mitosis. A wild-type strain containing Cdc5-HA (YMB9264) was grown at 30°C, arrested in G1 with α-factor, washed, and released into pheromone-free medium. α-Factor was added again 80 min after release to block the cells at the subsequent G1. Samples were taken at various time points (minutes) after G1 release. (A) FACS analysis revealed cell cycle progression. Cell cycle stages were determined based on cell morphology and nuclear position by microscopic examination of 100 cells for each time point. Different stages of the cell cycle: G1, S phase (S), metaphase (ME), anaphase (A), and telophase (T). (B) Expression of Cdc5 is cell cycle regulated. Western blot analysis was carried out on whole-cell protein extracts prepared from samples taken at various times after release from G1 arrest as in A. Blots were probed with α-HA (Cdc5) and α-Tub2 (loading control) antibodies. (C) Centromeric levels of Cdc5 are highest in mitotic cells. ChIP for Cdc5 was carried out using α-HA antibodies. Enrichment of Cdc5 at *CEN3* (top) and a negative control region *6K120* (bottom) determined by qPCR and shown as percentage input. Average from three biological replicates ± SE.

Next we examined whether Mcd1 is required for enrichment of Cdc5 at *CEN* and *CAR*s. Because cohesin subunits are essential for cell viability, we used *mcd1-1*, a well-characterized temperature-sensitive mutant that arrests in M phase at the nonpermissive temperature (37°C) and exhibits defects in establishment and maintenance of cohesion (Guacci *et al.*, 1997; Noble *et al.*, 2006; Skibbens *et al.*, 2010; Eng *et al.*, 2014, 2015). The expression of Cdc5 was similar in wild-type and *mcd1-1* strains grown at 25 and 37°C, as measured by Western blot analysis (Figure 7A). The enrichment of Cdc5 at *CEN* and *CAR*s in nocodazole-treated (M-phase arrest) wild-type and *mcd1-1* cells grown at 25°C and after shift to 37°C was assayed by ChIP. The cell cycle arrest was verified by FACS assay (Figure 7B). ChIP-qPCR showed that Cdc5 levels at *CEN3,* as well as *CAR*s located at *peri-CEN* (134) and the chromosomal arm (261), are reduced threefold to fourfold specifically in the *mcd1-1* strain at 37°C (Figure 7C). There was no significant enrichment of Cdc5 at negative control region *6K120* under any condition (Figure 7C). We conclude that cohesin is required for enrichment of Cdc5 at *CEN* and *CAR*s.

cdc5-99 strains exhibit persistence of cohesin at *CEN* and peri-*CEN* regions in anaphase

Given our findings that association of Cdc5 at centromeric chromatin and *CAR*s is maximal in cells undergoing the metaphase-to-anaphase transition (Figures 2 and 4), we posited that Cdc5 might be required for the removal of chromatin-bound cohesin. In wild-type cells, cohesin is lost from both centromeric chromatin and chromosomal arms at anaphase onset (Marston, 2014). To characterize the Cdc5 dependence of cohesin loss, we monitored the localization of Smc3-GFP in anaphase cells of wild-type and *cdc5-99* strains grown at permissive temperature (25°C) and after a 2.5-h shift to the nonpermissive temperature of 37°C. The well-characterized temperature-sensitive *cdc5-99* mutant exhibits a defect in mitotic exit at the nonpermissive temperature of 37°C (St-Pierre *et al.*, 2009). Spindle pole body (SPB) component Spc29–red fluorescent protein (RFP) was used as a marker for centromeric chromatin due to the close physical proximity of the SPB to the kinetochores in budding yeast. Using the distance between SPBs as a measure for spindle length, we quantitated Smc3-GFP foci in anaphase cells with a spindle length of 3–8 μm. In addition to the diffuse Smc3-GFP fluorescence observed over the separated chromatin masses in both wild-type and *cdc5-99* cells, distinct Smc3-GFP foci were observed in the *cdc5-99* mutant (Figure 8A). No detectable Smc3-GFP foci were ever observed in wild-type cells in anaphase. Quantification of the *cdc5-99* cells with Smc3-GFP foci at one or both of the spindle poles was significantly higher (32 vs. 13%, $p < 0.05$) at 37°C ($n = 144$) than at 25°C ($n = 125$; Figure 8B). We next examined the localization

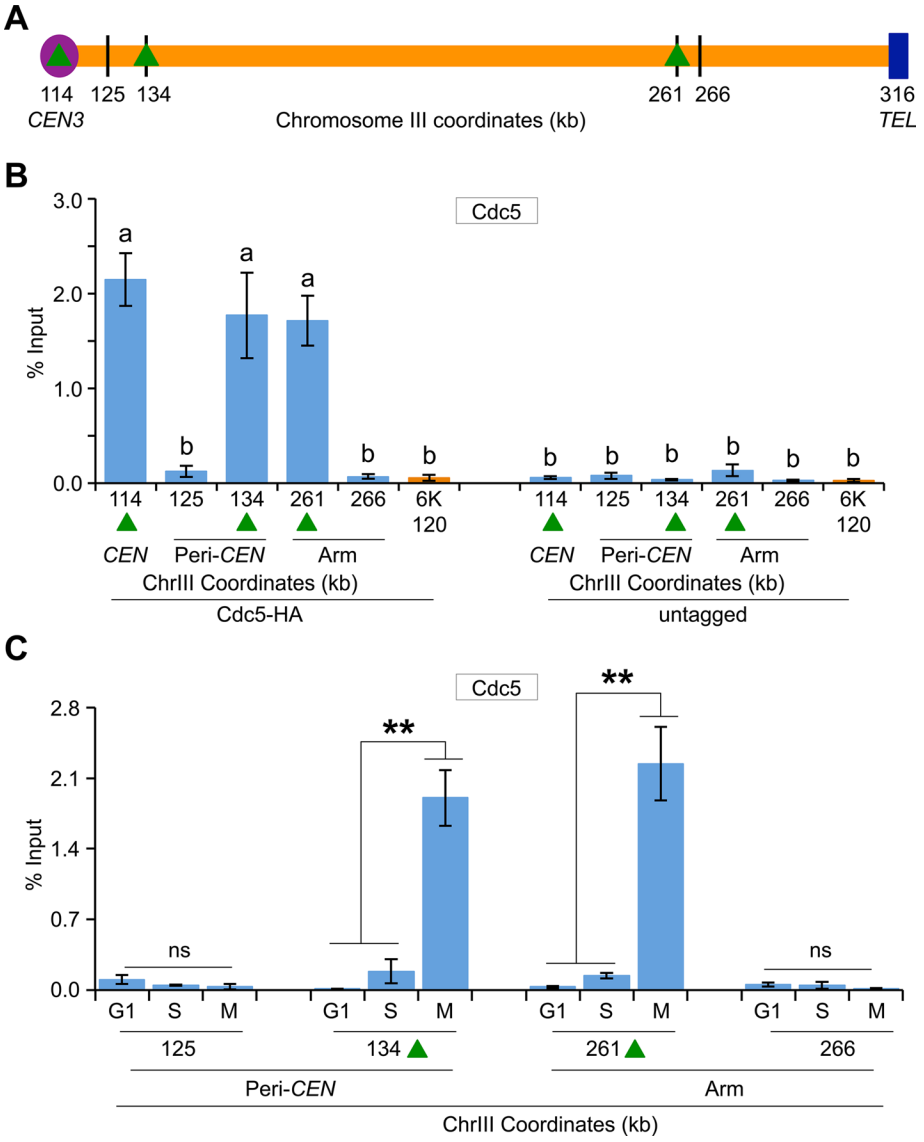

FIGURE 3: Cdc5 associates with *CAR*s in a cell cycle–dependent manner, with maximum enrichment in mitosis. (A) Schematic showing *CAR*s and non-*CAR*s on chromosome III. Cohesins have been shown to either associate (*CAR*s) or fail to associate (non-*CAR*s) at these regions in previous studies (Eckert *et al.*, 2007; Ng *et al.*, 2009). Centromere (*CEN3*, violet circle), *CAR* (green triangle), and non-*CAR* (black vertical line) sites. *CEN* is located at 114 kb; peri-*CEN CAR* 134 (20 kb from *CEN*), chromosome arm *CAR* 261 (147 kb from *CEN*), peri-*CEN* non-*CAR* 125 (11 kb from *CEN*), and chromosome arm non-*CAR* 266 (152 kb from *CEN*) were examined. (B) Cdc5 associates with *CAR*s. ChIP was performed for Cdc5 in a wild-type strain tagged with Cdc5-HA (YMB9264) and an untagged control strain (YMB9263). Cells were grown to logarithmic phase at 30°C. Enrichment of Cdc5 to *CEN* (114), *CAR* (134 and 261), and non-*CAR* control regions (125 and 266) on chromosome III was determined by qPCR and is shown as percentage input. Average values of three biological replicates ± SE of the mean. Values sharing the same letter (a, b) are not significantly different at the 5% level based on analysis of variance. (C) Enrichment of Cdc5 at *CAR*s is higher in mitotic cells. ChIP-qPCR was performed with wild-type strain YMB9264 (Cdc5-HA) using cells prepared as in Figure 1C. Enrichment at *CAR* (134 and 261) and non-CAR control (125 and 266) regions is shown as percentage input. Average from three biological replicates ± SE. $^{**}p < 0.01$; ns, not statistically significant, Student's *t* test.

pattern of another cohesin component, Mcd1-GFP, in anaphase cells of wild-type and *cdc5-99* strains using growth conditions and procedure as described earlier. The persistence of Mcd1-GFP foci was observed in anaphase cells of *cdc5-99* strain, whereas no detectable Mcd1-GFP foci were observed in wild-type cells (Figure 8C). The number of *cdc5-99* cells with Mcd1-GFP foci at one or both of the spindle poles was significantly higher (24 vs. 3%, $p < 0.05$) at 37°C ($n = 197$) than at 25°C ($n = 94$; Figure 8D).

The proximity of Smc3-GFP and Mcd1-GFP foci to Spc29-RFP in *cdc5-99* strains suggested the persistence of cohesin in centromeric chromatin; hence we used ChIP to assay the association of Smc3-HA at *CAR*s close to (*CEN*) or distant from the centromere (arm), using either metaphase or anaphase cells from wild-type, *cdc5-99*, and *cdc15-2* strains. Metaphase cells were obtained by growing strains at 25°C in nocodazole, and anaphase cells were obtained after release from nocodazole at the nonpermissive temperature of 37°C (Figure 9). We used *cdc15-2* as a control because this strain arrests at a stage similar to *cdc5* mutants during mitosis (Surana *et al.*, 1993; St-Pierre *et al.*, 2009). The cell cycle stage was determined by monitoring Pds1 levels (Cohen-Fix *et al.*, 1996) by Western blotting, DNA content by FACS, and nuclear morphology by microscopy (Calvert and Lannigan, 2010). High levels of Pds1 are present in metaphase; however, levels of Pds1 are undetectable in anaphase, as degradation of Pds1 is required for anaphase onset (Cohen-Fix *et al.*, 1996; Cohen-Fix and Koshland, 1999). Consistent with this, high levels of Pds1 were observed in metaphase but not in anaphase cells of wild-type, *cdc5-99*, and *cdc15-2* strains (Figure 9, A and B). Large-budded cells with the nucleus at the neck or separated nuclei indicate metaphase and anaphase cells, respectively (Figure 9B). ChIP-qPCR showed enrichment of Smc3-HA at *CEN* (114), *CAR*s flanking the centromere (112, 115), and the arms (261, 304, 307) in metaphase cells of wild-type, *cdc5-99*, and *cdc15-2* strains (Figure 9, C and D). Smc3-HA levels were significantly reduced at both the centromeric chromatin (*CEN* [114], peri-*CEN CAR*s [112, 115]) and the chromosomal arms (261, 304, 307) in anaphase cells of wild-type and *cdc15-2* strains, and these levels were largely similar to those at non-*CAR*s (125, 310; Figure 9D). In contrast, in anaphase cells of the *cdc5-99* strain, Smc3-HA levels were significantly reduced only at *CAR*s at chromosomal arms (261, 304, 307) and remained high at centromeric chromatin (*CEN* [114] and peri-*CEN CAR*s [112, 115]). The levels of Smc3-HA at *CEN* and peri-*CEN CAR*s in anaphase cells of *cdc5-99* strains were not statistically different from those observed at these chromosomal regions in metaphase cells (Figure 9D). No significant enrichment of Scm3-HA was detected at non-*CAR*s (125, 310) at either metaphase or anaphase (Figure 9D). These results suggest that Cdc5 is required for the removal of cohesin from centromeric chromatin during mitosis.

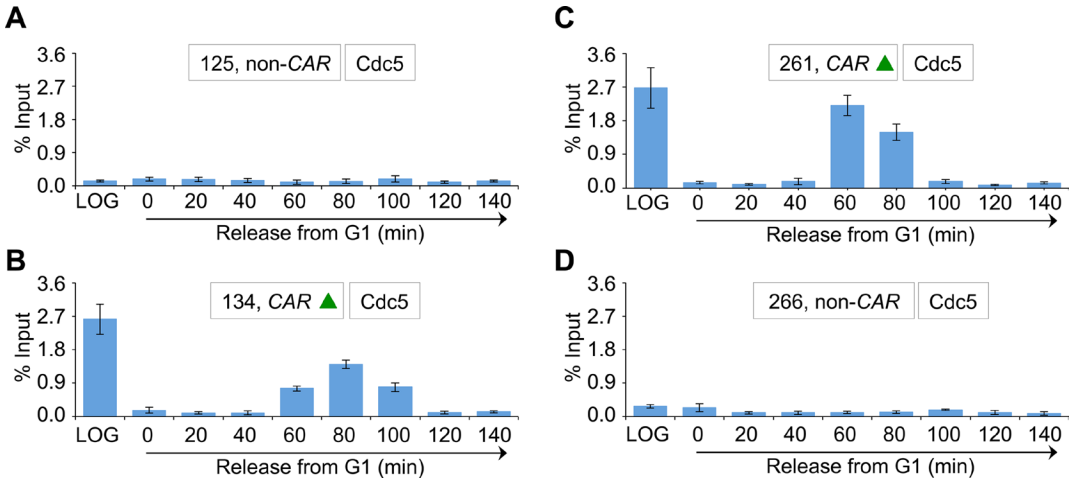

FIGURE 4: *CAR* association of Cdc5 is cell cycle regulated, with maximum enrichment in cells undergoing mitosis. A wild-type strain containing Cdc5-HA (YMB9264) was grown at 30°C, arrested in G1 with α-factor, washed, and released into pheromone-free medium. α-Factor was added again 80 min after release to block the cells at the subsequent G1. Samples were taken at various time points (minutes) after G1 release. ChIP-qPCR was performed to determine the enrichment pattern of Cdc5 at *CAR*s and non-*CAR*s on chromosome III throughout the cell cycle. The *CAR* (green triangles) and non-*CAR* (black vertical lines) examined are shown schematically in Figure 3A. Cdc5 enrichment is shown as percentage input. Average from three biological replicates ± SE for each time point. (A) Enrichment levels of Cdc5 at non-*CAR* (125) located at peri-*CEN3*. (B) Enrichment levels of Cdc5 at *CAR* (134) located at peri-*CEN3*. (C) Enrichment levels of Cdc5 at *CAR* (261) located at the chromosomal arm. (D) Enrichment levels of Cdc5 at non-*CAR* (266) located at the chromosomal arm.

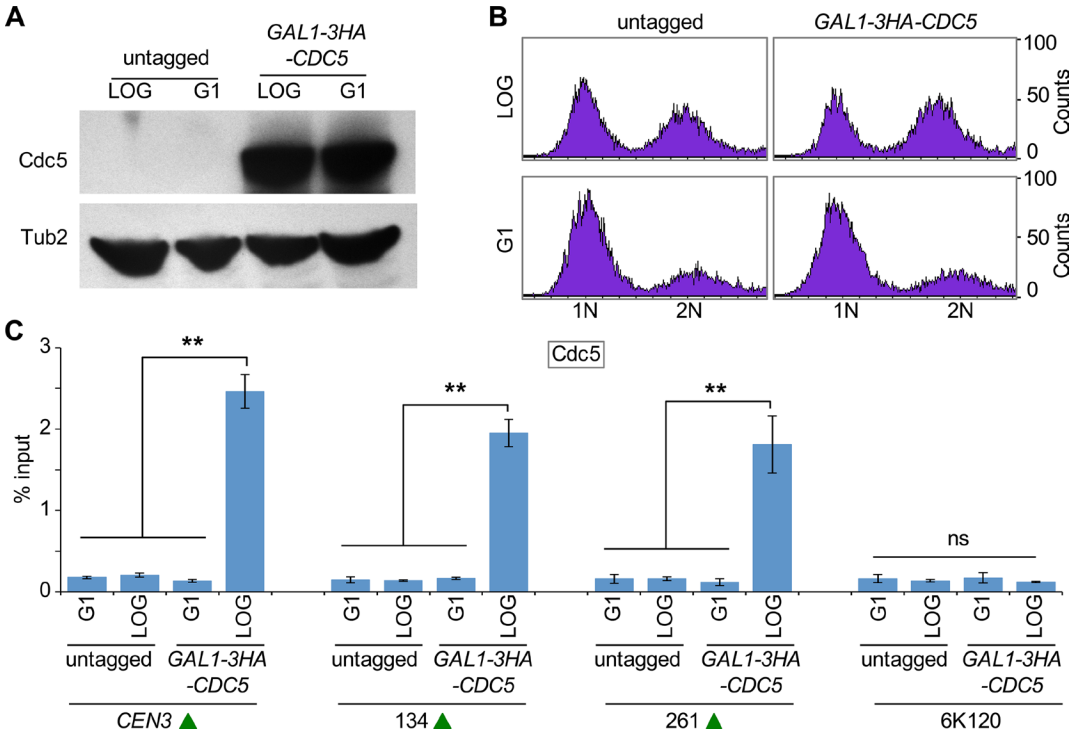

FIGURE 5: Induced expression of Cdc5 in G1 does not result in its recruitment to *CEN* and *CAR*s. A wild-type strain containing *GAL1-3HA-CDC5* (YMB9441) and untagged control (JG595) were grown at 30°C in yeast extract/peptone with 2% galactose and raffinose and arrested in G1 with α-factor for 2 h. Samples were collected for protein extraction, DNA content, and ChIP analyses. (A) Induced expression of Cdc5 (*GAL1-3HA-CDC5*) in G1. Western blot analysis was carried out on whole-cell protein extracts prepared from cultures growing logarithmically or arrested in G1 with α-factor treatment. Blots were probed with α-HA (Cdc5) and α-Tub2 (loading control) antibodies. (B) FACS analysis revealed synchronization of cells in G1. (C) Cdc5 does not associate with *CEN* and *CAR*s in G1. ChIP for Cdc5 (*GAL1-3HA-CDC5*) was carried out using α-HA antibodies. Enrichment of Cdc5 at *CEN3, CAR*s (134, 261), and a negative control region *6K120* was determined by qPCR and is shown as percentage input. Average from three biological replicates ± SE. $^{**}p < 0.01$; ns, not statistically significant, Student's *t* test.

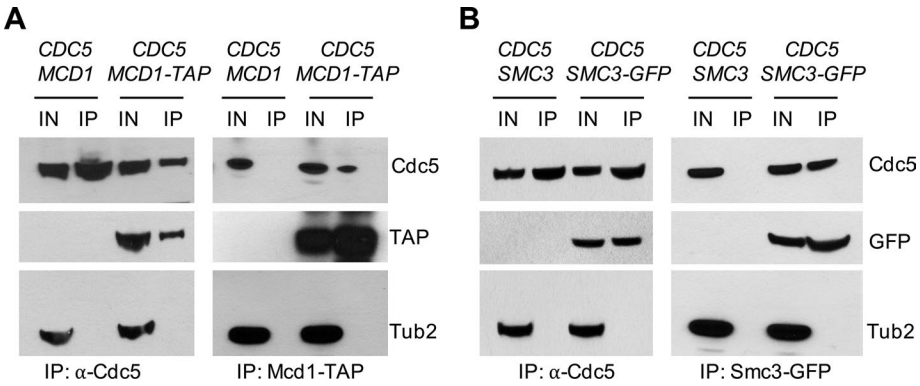

FIGURE 6: Cdc5 interacts with cohesin proteins Mcd1 and Smc3 in vivo. (A) Cdc5 interacts in vivo with Mcd1. Wild-type strain (MAY8878) expressing TAP-tagged Mcd1 (*CDC5 MCD1-TAP*) and a control strain (BY4741) expressing untagged Mcd1 (*CDC5 MCD1*) from their native promoters were grown at 30°C. Cell extracts were prepared and used in immunoprecipitation experiments using α-Cdc5 monoclonal and α-TAP antibodies. Eluted proteins were analyzed by Western blotting with α-Cdc5, α-TAP (Mcd1), and α-Tub2 (loading control) antibodies. IN, input; IP, immunoprecipitated samples. (B) Cdc5 interacts in vivo with Smc3. Wild-type strain (YMB9431) expressing GFP-tagged Smc3 (*CDC5 SMC3-GFP*) and a control strain (YMB8702) expressing untagged Smc3 (*CDC5 SMC3*) from their native promoters were grown at 30°C. Cell extracts were prepared and used in immunoprecipitation experiments using α-Cdc5 monoclonal and α-GFP antibodies. Eluted proteins were analyzed by Western blotting with α-Cdc5, α-GFP (Smc3), and α-Tub2 (loading control) antibodies.

A previous study showed that *SMC* subunits of cohesin complex (e.g., Smc1) remain associated with chromosomes for ~10 min after the degradation of Scc1/Mcd1 in anaphase (Tanaka *et al.*, 1999). Hence we investigated whether Cdc5 is also required for removal of Mcd1 from centromeric chromatin. We examined the association of Mcd1-HA at *CEN* and *CAR*s in *cdc5-99* and *cdc15-2* grown at 25°C in nocodazole (metaphase) and after release from nocodazole at 37°C (anaphase). We detected high levels of Pds1 in metaphase but not in anaphase cells of *cdc5-99*, and *cdc15-2* strains (Figure 10, A and B). The levels of Pds1 were slightly lower in *cdc15-2* than in the *cdc5-99* strain (Figure 10A). ChIP-qPCR showed enrichment of Mcd1-HA at *CEN* (114), *CAR*s flanking the centromere (112, 115), and the arms (261, 304, 307) in metaphase cells of *cdc5-99* and *cdc15-2* strains (Figure 10, C and D). Mcd1-HA levels were significantly reduced at *CEN* (114), peri-*CEN CAR*s (112, 115), and chromosomal arms *CAR*s (261, 304, 307) in anaphase cells of *cdc15-2*, and these levels were largely similar to those at non-*CAR*s (125, 31; Figure 10D). Consistent with the results for Smc3-HA, significantly reduced levels of Mcd1-HA were observed at *CAR*s in chromosomal arms (261, 304, 307), whereas Mcd1-HA levels remained high at centromeric chromatin (*CEN* [114] and peri-*CEN CAR*s [112, 115]) in anaphase cells of *cdc5-99* strains. The levels of Mcd1-HA at *CEN* and peri-*CEN CAR*s in anaphase cells of *cdc5-99* strains were statistically not different from those observed at these chromosomal regions in metaphase cells (Figure 10D). No significant enrichment of Mcd1-HA was detected at non-*CAR*s (125, 310) at either metaphase or anaphase (Figure 10D). The persistence of both Smc3 and Mcd1 in *CEN* and peri-*CEN* chromatin in anaphase cells of the *cdc5-99* strain supports a role for Cdc5 in the removal of cohesin from centromeric chromatin.

Cdc5 is required for faithful chromosome segregation

The cell cycle–regulated centromeric association of Cdc5 and its role in removal of centromeric cohesin led us to examine whether defects in Cdc5 would result in increased chromosome loss. We constructed a *cdc5-99* strain carrying a reporter chromosome (RC) and determined the frequency of loss of the RC using a colony color assay as described previously (Spencer *et al.*, 1990). Loss of the RC results in formation of red sectors in an otherwise white colony. Colonies that are at least half red indicate loss of the RC in the first cell division. The frequency of RC loss in *cdc5-99* strains was about sixfold higher than in the wild-type strain (Figure 11A), similar to that reported for kinetochore mutants (Kastenmayer *et al.*, 2005; Ma *et al.*, 2012).

DISCUSSION

Evolutionarily conserved polo-like kinase Cdc5 and its homologues play a range of crucial and conserved roles in regulation of cell cycle events (Alexandru *et al.*, 2001; Lee *et al.*, 2005; St-Pierre *et al.*, 2009; Rossio *et al.*, 2010; Ratsima *et al.*, 2011; Botchkarev *et al.*, 2014; Walters *et al.*, 2014; Zitouni *et al.*, 2014; Archambault *et al.*, 2015). Among its many roles, Cdc5 is required for the phosphorylation and subsequent cleavage of Scc1/Mcd1 in order to promote sister chromatid separation (Alexandru *et al.*, 2001; Hornig and Uhlmann, 2004). Our results provide mechanistic insight into the role of Cdc5 in the removal of centromeric cohesin during mitosis. We show that Cdc5 associates with centromeric chromatin and is required for the efficient removal of cohesin at core *CEN* and peri-*CEN* regions during mitosis. These conclusions are based on results showing that Cdc5: 1) associates with *CEN* and *CAR*s in a cell cycle–dependent manner, with maximum enrichment in mitosis; 2) interacts with cohesins in vivo; 3) requires cohesin for its mitotic enrichment at *CEN* and *CAR*s; 4) is required for the removal of cohesin from centromeric chromatin in anaphase; and 5) is required for faithful chromosome segregation.

Enrichment of Cdc5 at centromeric chromatin was highest in mitotic cells undergoing the transition from metaphase to anaphase. Even though Cdc5 is expressed in S-phase and anaphase cells, we observed significantly lower levels of chromatin-associated Cdc5 during the S phase of the cell cycle. Moreover, ectopic expression of Cdc5 in G1 does not result in its recruitment to *CEN* and *CAR*s, suggesting that the binding of Cdc5 to these chromosomal regions is regulated by the cell cycle. Association of Cdc5 flanking *CEN6* and *CAR*s was reported in a ChIP-on-chip study evaluating the role of Rsc2 in mitotic exit (Rossio *et al.*, 2010). Our comprehensive ChIP analysis shows that the cell cycle–regulated centromeric enrichment of Cdc5 coincides with its role in removal of cohesin from this region. We discovered that cohesin components Scc1/Mcd1 interact with Cdc5 in vivo, and the interaction is required for enrichment of Cdc5 at *CEN* and *CAR*s. It is of note that high-throughput proteomic studies also identified cohesin components when Cdc5 was used as bait in affinity-capture mass spectroscopy experiments (Ho *et al.*, 2002; Snead *et al.*, 2007; Breitkreutz *et al.*, 2010). The cohesin-dependent enrichment of Cdc5 at *CEN* and *CAR*s reflects a dynamic enzyme–substrate relationship between Cdc5 and cohesin components, resulting in preferential removal of chromatin-bound cohesin. Of most importance, our results suggest a role for Cdc5 in removal of centromeric cohesins, most likely from the intramolecular linkages in the C-loop (Yeh *et al.*, 2008; Hu *et al.*, 2011), but not cohesins in the arms of chromosomes (Figure 11B). The C-loop model resolved a paradox in which sister kinetochores can separate up to 800 nm in

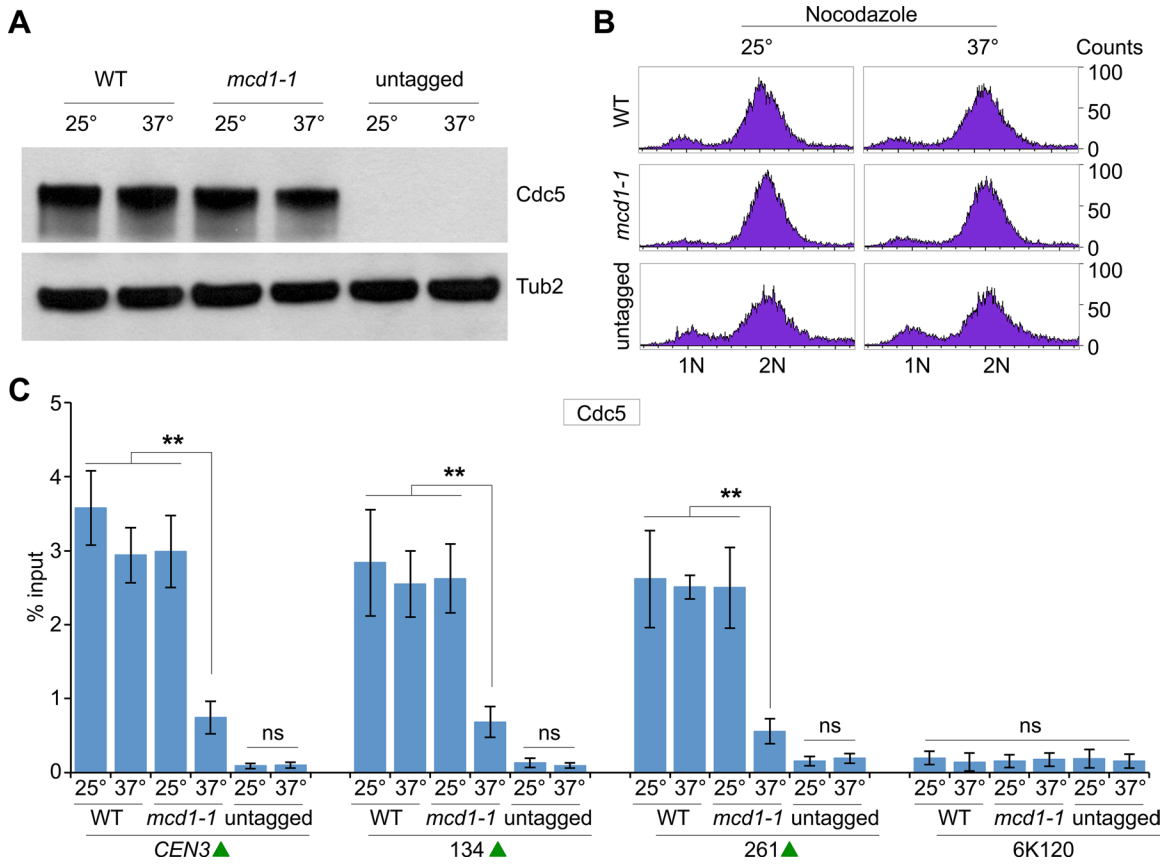

FIGURE 7: Mitotic enrichment of Cdc5 at *CEN* and *CAR*s requires cohesin. Wild type (WT; MAY8775), *mcd1-1* (MAY8851), and untagged control (YPH499) expressing Cdc5-13Myc were grown in YPD with nocodazole (20 µg/ml) to arrest cells in M phase at permissive temperature (25°C) and shifted to nonpermissive temperature (37°C) for 2.5 h. (A) Western blotting showing the protein expression levels of Cdc5 in WT, *mcd1-1*, and untagged control strains. Antibodies used were α-Myc (Cdc5) and α-Tub2 (loading control). (B) FACS profile showing synchronization of WT, *mcd1-1*, and untagged control strains in M phase of the cell cycle after nocodazole treatment. (C) Cdc5 levels are reduced at *CEN* and *CAR*s in *mcd1-1* strains. ChIP was performed using chromatin extracts from WT, *mcd1-1*, and untagged control strains with α-Myc antibodies. Enrichment of Cdc5 at the *CEN3* (114), peri-*CEN CAR* (134), and chromosomal arm *CAR* (261) was determined by qPCR and is shown as percentage input. *CAR*s are marked (green triangles). The negative control region *6K120* was used as a background control. Average from three biological replicates ± SE. $^{**}p < 0.01$; ns, not statistically significant, Student's *t* test.

vivo despite high levels of cohesin at centromeres. The persistence of Smc3 and Mcd1 in anaphase of *cdc5-99* cells at the nonpermissive temperature may reflect the presence of intramolecularly linked cohesin in the C-loop, whereas the absence of cohesin in chromosome arms shows that Cdc5 is dispensable for removal of intermolecularly linked cohesins. Cdc5 has been shown to regulate removal of cohesin from chromosome arms for segregation of homologous chromosomes in meiosis I but to be dispensable for meiosis II (Brar *et al.*, 2006; Katis *et al.*, 2010; Attner *et al.*, 2013). Attner *et al.* (2013) concluded that additional kinases or substrates and/or the differential nature of centromeric versus chromosome arm cohesin regulate the removal of centromeric cohesin in meiosis II. On the basis of our results, we conclude that Cdc5 represents the first example of differential regulation of centromeric versus arm cohesin during mitosis in budding yeast.

The mitotic enrichment of Cdc5 at *CEN* suggests a role for Cdc5 in kinetochore function because of major changes in spatial geometry and spindle tension that occur at the kinetochore during mitosis. Consistent with this hypothesis, we observed errors in chromosome segregation in the *cdc5-99* strain. Because Cdc5 is involved in many biological processes (Archambault and Glover, 2009; St-Pierre *et al.*, 2009; Botchkarev *et al.*, 2014; Walters *et al.*, 2014; Zitouni *et al.*, 2014; Roccuzzo *et al.*, 2015), chromosome segregation errors observed in *cdc5-99* strain may not be due to solely defects in cohesin removal. Previous studies showed that Cdc5 interacts with and phosphorylates kinetochore proteins in vivo (e.g., Slk19) to promote proper microtubule attachment and spindle function (Stegmeier *et al.*, 2002; Snead *et al.*, 2007; Park *et al.*, 2008; Liang *et al.*, 2009; Richmond *et al.*, 2013). Plk1, the human homologue of Cdc5, also localizes to the *CEN* (Arnaud *et al.*, 1998; Kishi *et al.*, 2009), where it likely phosphorylates Rad21 (the human Scc1 homologue; Waizenegger *et al.*, 2000). In addition, Plk1 phosphorylates kinetochore protein Mis18BP1, which in turn licenses the recruitment of new CENP-A to kinetochores in the G1 phase of the cell cycle (McKinley and Cheeseman, 2014). Of note, Cse4 (the budding yeast CENP-A homologue) was identified as an in vivo interacting partner of Cdc5 in a genome-wide proteomic study (Snead *et al.*, 2007). Future studies should help us to address whether Cdc5-mediated phosphorylation of kinetochore proteins affects the removal of centromeric cohesins.

In summary, our studies provide novel insights into the role of Cdc5 in removal of centromeric cohesin but not cohesin from

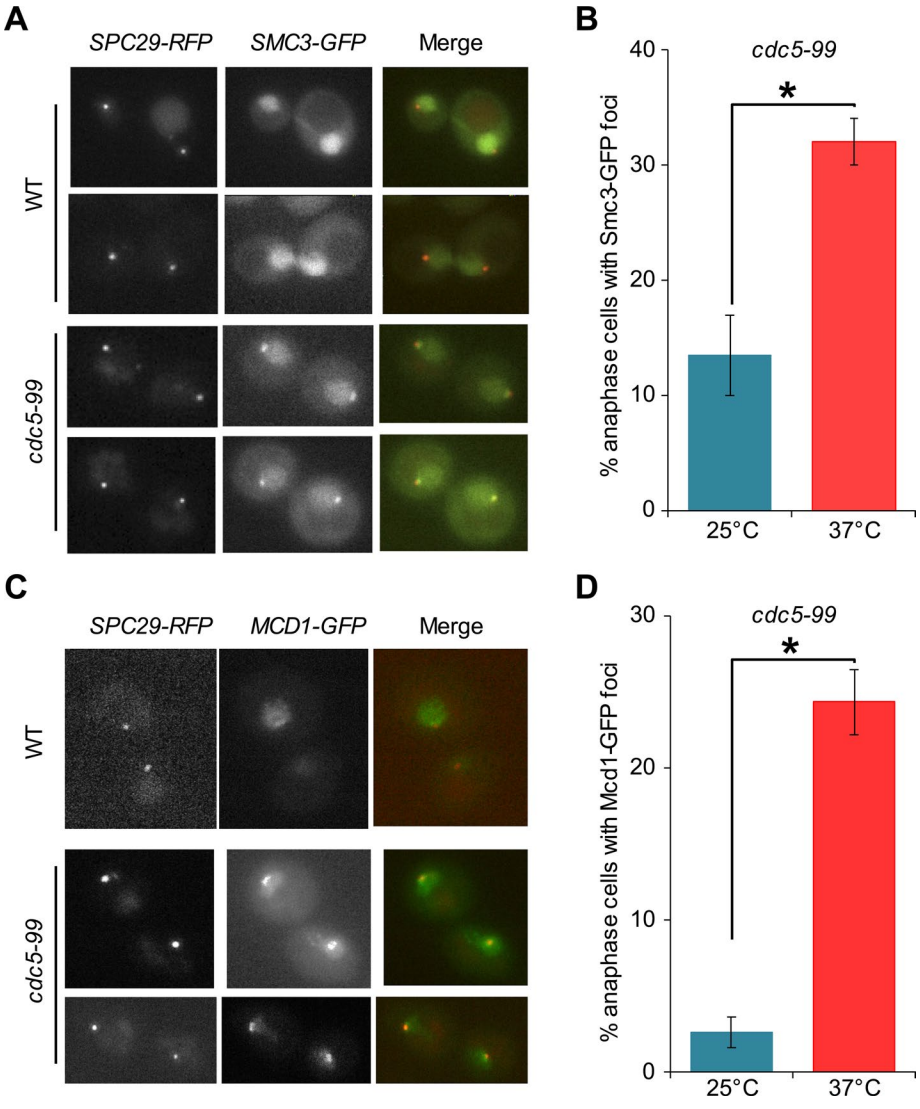

FIGURE 8: Persistence of Smc3 and Mcd1 close to spindle pole bodies in anaphase cells of *cdc5-99* strains. (A) Wild-type (WT, KBY6098-1) and *cdc5-99* (KBY6097-1) strains containing *SMC3-GFP* and *SPC29-RFP* were grown at permissive temperature (25°C) and shifted to the nonpermissive temperature (37°C) for 2.5 h. Cells with spindle length 3–8 µm were considered to be in anaphase and were used for imaging. Spc29-RFP was used as a spindle pole marker. Representative images showing the persistence of Smc3-GFP signals in anaphase cells of *cdc5-99* strain (KBY6097-1). (B) Percentage of Smc3-GFP foci proximal to the spindle poles was determined in *cdc5-99* strain (KBY6097-1) at permissive temperature (25°C, $n = 125$) and 2.5 h after shift to nonpermissive temperature (37°C, $n = 144$). Standard weighted-means analysis was used to calculate averages, and significance was determined by one-way analysis of variance. Bar diagram represents average ± SE of the mean. *$p < 0.05$. (C) WT (YMB9695) and *cdc5-99* (YMB9696) strains containing *MCD1-GFP* and *SPC29-RFP* were used. Strain VG3507-2A carrying *MCD1-GFP* (a gift from Vincent Guacci, University of California, Berkeley, CA) was used to construct strains YMB9695 and YMB9696. Strains were grown at permissive temperature (25°C) and shifted to the nonpermissive temperature (37°C) for 3 h. Cells with spindle length 3–8 µm were considered to be in anaphase and were used for imaging. Spc29-RFP was used as a spindle pole marker. Representative images showing the persistence of Mcd1-GFP signals in anaphase cells of *cdc5-99* strain (YMB9696). (D) Percentage of Mcd1-GFP foci proximal to the spindle poles was determined in *cdc5-99* strain (YMB9696) at permissive temperature (25°C, $n = 94$) and 3 h after shift to nonpermissive temperature (37°C, $n = 197$). Standard weighted-means analysis was used to calculate averages, and significance was determined by one-way analysis of variance. Bar diagram represents average ± SE of the mean. *$p < 0.05$.

chromosomal arms. Differential regulation of cohesin removal has also been reported in mammalian cells, where removal of cohesin from chromosomal arms in prometaphase is regulated by the cohesin antagonist *WAPL*, whereas removal of centromeric cohesin at the metaphase-to-anaphase transition by Plk1 is achieved by a separase-dependent mechanism (Waizenegger *et al.*, 2000; Hauf *et al.*, 2001; Gandhi *et al.*, 2006; Kueng *et al.*, 2006; Haarhuis *et al.*, 2013). Mutations and overexpression of Plk1 are observed in many cancers (Davies *et al.*, 2005; Stephens *et al.*, 2005; Kan *et al.*, 2010), displaying chromosomal instability and aneuploidy (Degenhardt and Lampkin, 2010). Hence elucidation of molecular mechanisms by which polo kinases regulate cohesin removal and faithful chromosome segregation might help us identify and develop novel therapeutic targets for cancer therapy.

MATERIALS AND METHODS

Strains, plasmids, and culture conditions

Saccharomyces cerevisiae strains and plasmids used in this study are listed in Table 1. Strains were grown in 1% yeast extract/2% Bacto-peptone/2% glucose (YPD) or in yeast synthetic medium containing 2% glucose and supplements to allow for the selection of plasmids used.

Assay for the loss of reporter chromosome

Loss of a nonessential RC was measured using a colony color assay in which RC loss results in red sectors in an otherwise white colony (Spencer *et al.*, 1990). Wild-type and *cdc5-99* strains were grown to logarithmic phase in selective medium to maintain the RC. Cultures were diluted and plated on complete synthetic medium with limiting adenine at 30°C. The frequency of chromosome loss was measured by counting the colonies that were at least half red, indicating loss of the RC at the first cell division. At least 3000 colonies of three individual transformants were examined for each strain.

ChIP and qPCR experiments

ChIP assays were performed with three biological replicates as described previously (Mishra *et al.*, 2007, 2011). Antibodies used to capture protein–DNA complexes were α-HA (A2095; Sigma-Aldrich, St. Louis, MO) and α-Myc (A7470; Sigma-Aldrich). ChIP-qPCR was carried out using SYBR Green Master Mix in a 7500 Fast Real Time PCR System (Applied Biosystems, Foster City, CA) following conditions used previously (Mishra *et al.*, 2011). The enrichment values were determined as percentage input using the $\Delta\Delta C_T$ method (Livak and Schmittgen, 2001). Primer sequences used in this study are presented in Table 2.

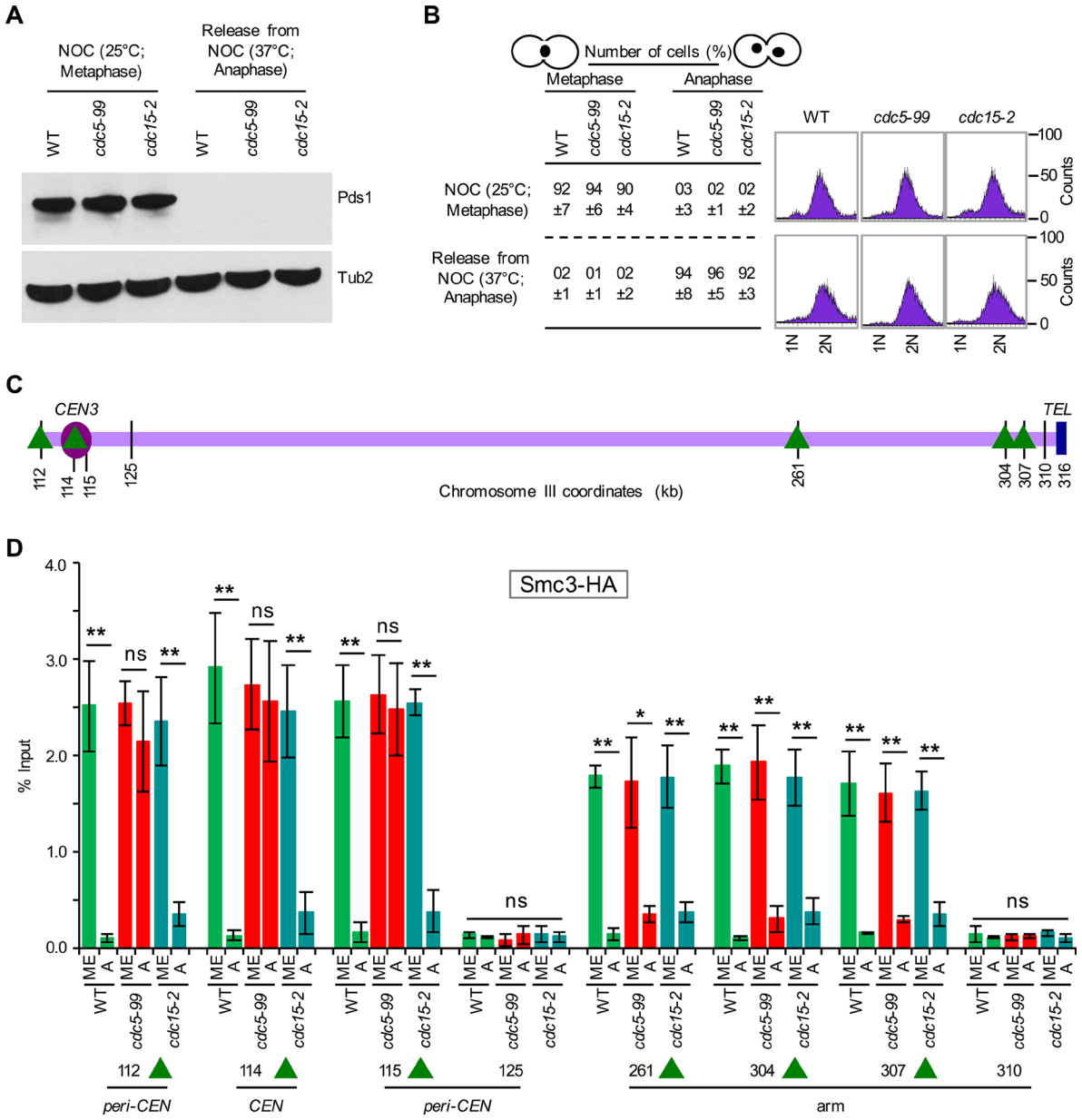

FIGURE 9: Cdc5 is required for the removal of Smc3 from centromeric chromatin. WT (YMB9693), *cdc5-99* (YMB9709), and *cdc15-2* (YMB9703) expressing Smc3-6HA and Pds1-18Myc from their endogenous promoters were used. Smc3-6HA was an internally tagged version of Smc3 (six copies of HA inserted at amino acid residue 607) using plasmid pVG466 (a gift from Vincent Guacci). Strains were grown in YPD at permissive temperature (25°C) with nocodazole (NOC, 20 µg/ml) for 2 h to synchronize cells in metaphase. Cells were then shifted to nonpermissive temperature (37°C) for 1 h, followed by release from NOC into YPD at 37°C for 45 min to enrich cells in anaphase. Samples were collected for Western blot analysis for Pds1, nuclear morphology, DNA content, and ChIP analyses. Three biological replicates were performed for each strain. (A) Western blot analysis showing high levels of Pds1 only in metaphase cells of WT, *cdc5-99*, and *cdc15-2* strains. Antibodies used were α-Myc (Pds1) and α-Tub2 (loading control). (B) Cell cycle stages (metaphase and anaphase) were determined based on nuclear position and cell morphology by microscopic examination of 100 cells for each strain per replicate as described previously (Calvert and Lannigan, 2010; Mishra *et al.*, 2011). DNA content was determined by FACS. (C) Schematic representation of *CAR*s and non-*CAR*s on chromosome III. The schematic is derived from Figure 3A with additional *CAR*s and non-*CAR*s. Centromere (*CEN3*, violet circle), *CAR* (green triangle), and non-*CAR* (black vertical line) sites. *CEN* is located at 114 kb; peri-*CEN* *CAR*s 115 (1 kb from *CEN*) and 112 (2 kb from *CEN*), chromosome arm *CAR* 261 (147 kb from *CEN*), 304 (190 kb from *CEN*), 307 (193 kb from *CEN*), peri-*CEN* non-*CAR* 125 (11 kb from *CEN*), and chromosome arm non-*CAR* 310 (196 kb from *CEN*) were examined. (D) Smc3 persists at *CEN* and peri-*CEN* chromatin in *cdc5-99* strains. ChIP was performed with chromatin prepared from metaphase (ME) or anaphase (A) with strains as described using α-HA antibodies. Enrichment of Smc3 at *CEN3* (114), peri-*CEN* *CAR*s (112, 115), and chromosomal arm *CAR*s (261, 304, 307) were determined by qPCR and is shown as percentage input. The non-*CAR* peri-*CEN* loci 125 and 310 in chromosome arms were used as a negative control. Average from three biological replicates ± SE. $^{**}p < 0.01$; $^{*}p < 0.05$; ns, not significant, Student's *t* test.

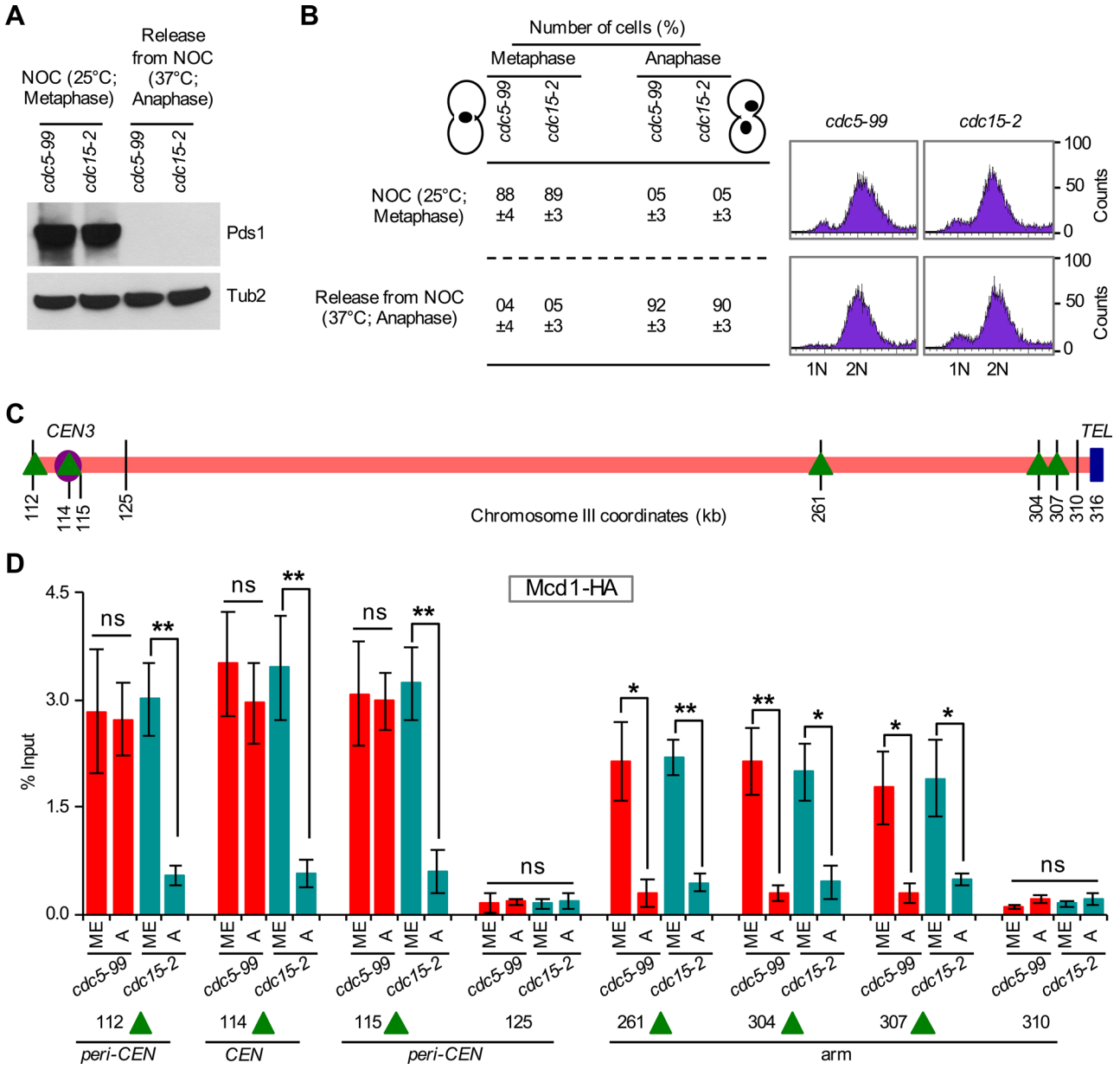

FIGURE 10: Cdc5 is required for the removal of Mcd1 from centromeric chromatin. *cdc5-99* (YMB9711), and *cdc15-2* (YMB9712) strains expressing Mcd1-3HA, and Pds1-18Myc from their endogenous promoters were used. Strains KT046 (Tong and Skibbens, 2014) and D1469 carrying *MCD1-3HA* were used to construct strains YMB9711 and YMB9712, respectively. Strains were grown in YPD at permissive temperature (25°C) with nocodazole (NOC; 20 µg/ml) for 2 h to synchronize cells in metaphase. Cells were then released into YPD at nonpermissive temperature (37°C) for 2.5 h to enrich cells in anaphase. Samples were collected for Western blot analysis, nuclear morphology, DNA content, and ChIP analyses. Three biological replicates were performed for each strain. (A) Western blotting showing high levels of Pds1 only in metaphase cells of *cdc5-99* and *cdc15-2* strains. Antibodies used were α-Myc (Pds1) and α-Tub2 (loading control). (B) Cell cycle stages (metaphase and anaphase) were determined based on nuclear position and cell morphology by microscopic examination of 100 cells for each strain per replicate. DNA content was determined by FACS. (C) Schematic representation of *CAR*s and non-*CAR*s on chromosome III as detailed in Figure 9C. (D) Mcd1 persists at *CEN* and peri-*CEN* chromatin in *cdc5-99* strains. ChIP experiments were performed using chromatin prepared from metaphase (ME) or anaphase (A) cells from strains as described using α-HA antibodies. Enrichment of Mcd1 at *CEN3* (114), peri-*CEN CAR*s (112, 115), and chromosomal arm *CAR*s (261, 304, 307) were determined by qPCR and is shown as percentage input. The non-*CAR* peri-*CEN* loci 125 and 310 in chromosome arms were used as negative controls. Average from three biological replicates ± SE. $^{**}p < 0.01$; $^{*}p < 0.05$; ns, not significant, Student's *t* test.

Immunoprecipitation and Western blotting

Immunoprecipitation assays were performed as described previously (Mishra *et al.*, 2011). Protein extracts were prepared with the trichloroacetic acid procedure and quantified using the Bio-Rad DC protein assay (Bio-Rad Laboratories, Hercules, CA). Equal amounts of protein for each sample were resolved on

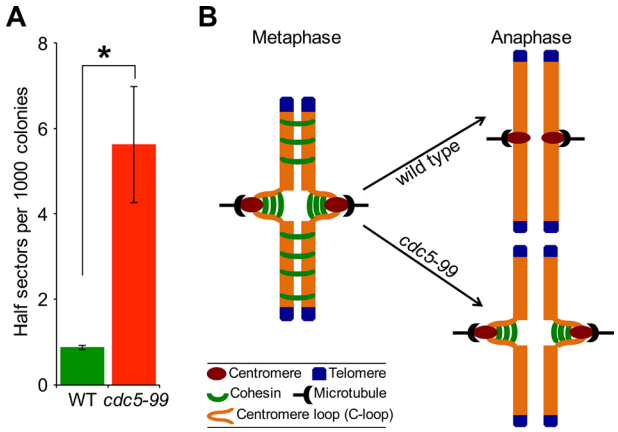

FIGURE 11: Cdc5 is required for faithful chromosome segregation. (A) Cdc5 is required for faithful chromosome segregation. Frequency of RC loss in wild-type (WT; YPH363) and *cdc5-99* (YMB9438) strains was determined as described in *Materials and Methods*. At least 3000 colonies from three independent transformants were counted. Values are mean ± SE. *$p < 0.05$, Student's *t* test. (B) Schematic model for the role of Cdc5 in cohesin removal from centromeric chromatin during mitosis. In WT cells, cohesin is removed from chromosomal arms and centromeric chromatin during metaphase-to-anaphase transition, whereas in *cdc5-99* strains, cohesin is removed from chromosomal arms but persists at centromeric chromatin.

SDS–polyacrylamide gels and transferred to nitrocellulose membrane. Primary antibodies used were α-HA (clone 12CA5; Roche Molecular Systems, Pleasanton, CA), α-GFP (A11122; Life Technologies, Carlsbad, CA), α-TAP (CAB1001; Thermo Scientific, Waltham, MA), α-Cdc5 (11H12 and 4F10; Medimabs, Montreal, Canada), α-Myc (Z-5, sc-789; Santa Cruz Biotechnology, Dallas, TX), and α-Tub2 (Mishra *et al.*, 2011). Secondary antibodies were horseradish peroxidase (HRP)–conjugated donkey α-rabbit immunoglobulin G (IgG; NA934V, Amersham Biosciences, Amersham, United Kingdom), and HRP-conjugated sheep α-mouse IgG (NA931V; Amersham Biosciences).

Microscopy

Cultures grown to logarithmic phase at permissive temperature (25°C) and after a shift to nonpermissive temperature (37°C) were used for all imaging experiments. Anaphase cells that exhibited a spindle length of 3–8 μm were selected based on the position of spindle pole bodies (Spc29-RFP; Chen *et al.*, 2000; Maddox *et al.*, 2000). Cells were imaged for Smc3-GFP, Mcd1-GFP, and Spc29-RFP signals at room temperature on a Nikon TE-2000E inverted microscope equipped with a 1.4 numerical aperture/100× Plan-Apo objective (Nikon Instruments, New York, NY) as described previously (Haase *et al.*, 2013; Salmon *et al.*, 2013).

Strain name	Genotype	Reference
YMB9431	*MATa ura3-1 leu2-3112 his3-11,15 trp1-1 ade2-1 can1-100 SMC3-GFP::URA3*	This study
YMB9263	*MATa ura3-52 lys2-801 ade2-101 trp1Δ63 his3Δ200 leu2Δ1 CSE4-13MYC::LEU2 CEN-TRP1*	This study
YMB9264	*MATa ura3-52 lys2-801 ade2-101 trp1Δ63 his3Δ200 leu2Δ1 CSE4-13MYC::LEU2 CEN-CDC5-3HA::TRP1 (p344)*	This study
JG595	*MATa ura3-1 leu2,3-112 his3-1 trp1-1 ade2-1 can1-100 Δbar1 CSE4-12MYC::URA3 SCM3-3FLAG::kanMX*	Camahort *et al.* (2007)
YMB9441	*MATa ura3-1 leu2,3-112 his3-1 trp1-1 ade2-1 can1-100 Δbar1 CSE4-12Myc::URA3 SCM3-3FLAG::kanMX GAL1-3HA-CDC5::TRP1*	This study
YMB9693	*MATa ura3-1 leu2-3112 his3-11,15 trp1-1 ade2-1 can1-100 SMC3-N607-6HA::URA3 PDS1-18MYC::LEU2*	This study
YMB9695	*MATa MCD1-GFP leu2-3112 ura3-52 his3-11,15 bar1 GAL+ SPC29-RFP::Hyg*	This study
YMB9696	*MATa MCD1-GFP leu2-3112 ura3-52 his3-11,15 bar1 GAL+ SPC29-RFP::Hyg cdc5-99::HIS3MX6*	This study
YMB9703	*MATa ura3-1 leu2-3112 his3-11,15 trp1-1 ade2-1 can1-100 SMC3-N607-6HA::URA3 PDS1-18MYC::LEU2 cdc15-2*	This study
YMB9709	*MATa ura3-1 leu2-3112 his3-11,15 trp1-1 ade2-1 can1-100 SMC3-N607-6HA::URA3 PDS1-18MYC::LEU2 cdc5-99::HIS3MX6*	This study
YMB9711	*MATa ade2-1 his3-11,15 leu2-3112 trp1-1 ura3-1 can1-100 MCD1-3HA::TRP1 PDS1-18MYC::LEU2 cdc5-99::HIS3MX6*	This study
YMB9712	*MATα leu2-3112 trp1-1 can1-100 ura3-1 ade2-1 his3-11,15 [phi+] rad5-535 MCD1-3HA::HPHMX6 cdc15-2::TRP1 PDS1-18MYC::LEU2*	This study
YMB8702	*MATa ura3-1 leu2-3112 his3-11,15 trp1-1 ade2-1 can1-100*	This study
KBY6097-1	*MATα ura3-1 leu2-3112 his3-11,15 trp1-1 ade2-1 can1-100 SMC3-GFP::URA3 cdc5-99::HIS3MX6 SPC29-RFP::Hyg*	This study
KBY6098-1	*MATa ura3-1 leu2-3112 his3-11,15 trp1-1 ade2-1 can1-100 SMC3-GFP::URA3 SPC29-RFP::Hyg*	This study
YMB9438	*MATα ura3-52 lys2-801 leu2-Δ1 ade2-101 his3-Δ200 [CFIII (CEN3.L) CFVII (RAD2.d) URA3 SUP11] cdc5-99::HIS3*	This study
YPH363	*MATα ura3-52 lys2-801 leu2-Δ1 ade2-101 his3-Δ200 [CFIII (CEN3.L) CFVII (RAD2.d) URA3 SUP11]*	Spencer *et al.* (1990)

TABLE 1: Strains and plasmids used in this study.

Continues

Strain name	Genotype	Reference
BY4741	*MATa ura3Δ0 leu2Δ0 his3Δ1 met15Δ0*	Open Biosystems, Lafayette, CO
MAY8878	*MATa his3Δ1 leu2Δ0 met15Δ0 ura3Δ0 MCD1-TAP::HIS3*	This study
YPH499	*MATa ura3-52 lys2-801 ade2-101 trp1Δ63 his3Δ200 leu2Δ1*	Sikorski and Hieter (1989)
MAY8775	*MATa ura3-52 ade2-101 his3-11,15 leu2-3112 CDC5-13MYC*	This study
MAY8851	*MATa ura3-52 ade2-101 his3-11,15 leu2-3112 CDC5-13MYC mcd1-1*	This study
VG3507-2A	*MATa MCD1-GFP leu2-3112 ura3-52 his3-11,15 bar1 GAL+*	V. Guacci, University of California, Berkeley, CA
KT046	*MATa ade2-1 his3-11,15 leu2-3112 trp1-1 ura3-1 can1-100 MCD1-3HA::TRP1*	Tong and Skibbens (2014)
D1469	*MATα leu2-3112 trp1-1 can1-100 ura3-1 ade2-1 his3-11,15 [phi+] rad5-535 MCD1-3HA::HPHMX6 cdc15-2::TRP1*	D. D'Amours, Université de Montréal, Montréal, QC
Plasmids	**Description**	**Reference**
p344	*CEN-CDC5-3HA::TRP1*	D. D'Amours
pVG466	*SMC3-N607-6HA::URA3*	V. Guacci
pSB205	*PDS1-18MYC::LEU2*	S. Biggins, Fred Hutchinson Cancer Research Center, Seattle, WA

TABLE 1: Strains and plasmids used in this study. Continued

Locus	Forward (5′–3′)	Reverse (5′–3′)	Reference
CEN1	CTCGATTTGCATAAGTGTGCC	GTGCTTAAGAGTTCTGTACCAC	Choy *et al.* (2011)
CEN3	GATCAGCGCCAAACAATATGG	AACTTCCACCAGTAAACGTTTC	Choy *et al.* (2011)
CEN5	AAGAACTATGAATCTGTAAATGACTGATTCAAT	CTTGCACTAAACAAGACTTTATACTACGTTTAG	Choy *et al.* (2011)
6K120	AACGTCACTTTTTTTCCAGGG	GCAAAGCTAGCTAACGAACAA	This study
CEN3-L1	ATATTGTTTGGCGCTGATCGCC	TTGATGAACTTTTCAAAGATGAC	Choy *et al.* (2011)
CEN3-L2	TCATCTTTGAAAAGTTCATCAAGG	GATAACAAAGCATGGTATGGCG	Choy *et al.* (2011)
CEN3-L3	GCCATACCATGCTTTGTTATCGTC	TATTATGCTCCCCTGGATTTTATGCG	Choy *et al.* (2011)
CEN3-L4	AGCATTAGAGCCACTGTCATTTC	ATAATTAAGATACGAATGTGTTCGTTG	Mishra *et al.* (2013)
CEN3-R1	TTTACTGGTGGAAGTTTTGCTCA	GTCAACGAGTCCTCTCTGGCTA	Choy *et al.* (2011)
CEN3-R2	GAGAGGACTCGTTGACGTAGAA	GAATATGATAATGGTTACACCAGTAGG	Choy *et al.* (2011)
CEN3-R3	TGTAACCATTATCATATTCATGAC	GATTTAATGCACGTTATGTTTCG	Choy *et al.* (2011)
CEN3-R4	ACTGACAGCACCATTAATCAATCA	TATCCTCAGTAGAGGGCAAAGTT	Mishra *et al.* (2013)
125	TGCCAAGTTGTGCTTTTTAGTTGAG	TTGATGTGTTGATTGTTCGGTCAC	Eckert *et al.* (2007), Ng *et al.* (2009)
134	CCGATGGTTAGGATTTCCAACG	GGTTTTCAGAACAGAATGGGGC	Eckert *et al.* (2007), Ng *et al.* (2009)
261	TTGCCACAGCCACAGATATAACTG	GATGGACAAAGCGTTGTATCCG	Eckert *et al.* (2007), Ng *et al.* (2009)
266	CAGACTTCCTCCAAGCAACAGG	TCCTCCTTAGCCTTTTCTTCAGC	Eckert *et al.* (2007), Ng *et al.* (2009)
304	CCCCTTCCAAAGACCTGACA	CCAGCCGTCGATCCTAAAGA	Laloraya *et al.* (2000)
307	GTAGCGCTCTCAACTACCCT	TCGTATACTGTTAGGGTCTGCA	Laloraya *et al.* (2000)
310	TCTCGGAATTTATCATGACCCAT	AAACCCTGCACACATTTCGT	Laloraya *et al.* (2000)

TABLE 2: Primers used in this study.

ACKNOWLEDGMENTS

We are highly thankful to Vincent Guacci and Robert Skibbens for strains, plasmids, and helpful suggestions. We thank Sue Biggins for plasmids and Jennifer Gerton for strains, Kathy McKinnon of the National Cancer Institute Vaccine Branch FACS Core for assistance with FACS and the Basrai laboratory for discussions. P.K.M., S.C.Y., W.C.A., L.B., L.E.D., Z.J., T.P., and M.A.B. were supported by the Intramural Research Program of the National Cancer Institute, National Institutes of Health; M.A.H. and D.R. by the National Science Foundation; E.Y. and K.B. by the National Institutes of Health (R37 GM32238); and D.D. by the Cancer Research Society and the Canadian Institutes of Health Research (MOP 82912).

REFERENCES

Alexandru G, Uhlmann F, Mechtler K, Poupart MA, Nasmyth K (2001). Phosphorylation of the cohesin subunit Scc1 by Polo/Cdc5 kinase regulates sister chromatid separation in yeast. Cell 105, 459–472.

Archambault V, Glover DM (2009). Polo-like kinases: conservation and divergence in their functions and regulation. Nat Rev Mol Cell Biol 10, 265–275.

Archambault V, Lepine G, Kachaner D (2015). Understanding the Polo kinase machine. Oncogene 34, 4799–4807.

Arnaud L, Pines J, Nigg EA (1998). GFP tagging reveals human Polo-like kinase 1 at the kinetochore/centromere region of mitotic chromosomes. Chromosoma 107, 424–429.

Attner MA, Miller MP, Ee LS, Elkin SK, Amon A (2013). Polo kinase Cdc5 is a central regulator of meiosis I. Proc Natl Acad Sci USA 110, 14278–14283.

Blat Y, Kleckner N (1999). Cohesins bind to preferential sites along yeast chromosome III, with differential regulation along arms versus the centric region. Cell 98, 249–259.

Bloom KS, Amaya E, Carbon J, Clarke L, Hill A, Yeh E (1984). Chromatin conformation of yeast centromeres. J Cell Biol 99, 1559–1568.

Bloom KS, Carbon J (1982). Yeast centromere DNA is in a unique and highly ordered structure in chromosomes and small circular minichromosomes. Cell 29, 305–317.

Bose T, Gerton JL (2010). Cohesinopathies, gene expression, and chromatin organization. J Cell Biol 189, 201–210.

Botchkarev VV Jr, Rossio V, Yoshida S (2014). The budding yeast Polo-like kinase Cdc5 is released from the nucleus during anaphase for timely mitotic exit. Cell Cycle 13, 3260–3270.

Brar GA, Kiburz BM, Zhang Y, Kim JE, White F, Amon A (2006). Rec8 phosphorylation and recombination promote the step-wise loss of cohesins in meiosis. Nature 441, 532–536.

Breitkreutz A, Choi H, Sharom JR, Boucher L, Neduva V, Larsen B, Lin ZY, Breitkreutz BJ, Stark C, Liu G, *et al.* (2010). A global protein kinase and phosphatase interaction network in yeast. Science 328, 1043–1046.

Brooker AS, Berkowitz KM (2014). The roles of cohesins in mitosis, meiosis, and human health and disease. Methods Mol Biol 1170, 229–266.

Burrack LS, Berman J (2012). Flexibility of centromere and kinetochore structures. Trends Genet 28, 204–212.

Calvert ME, Lannigan J (2010). Yeast cell cycle analysis: combining DNA staining with cell and nuclear morphology. Curr Protoc Cytom Chapter 9, Unit 9.32.1–16.

Camahort R, Li B, Florens L, Swanson SK, Washburn MP, Gerton JL (2007). Scm3 is essential to recruit the histone h3 variant cse4 to centromeres and to maintain a functional kinetochore. Mol Cell 26, 853–865.

Charles JF, Jaspersen SL, Tinker-Kulberg RL, Hwang L, Szidon A, Morgan DO (1998). The Polo-related kinase Cdc5 activates and is destroyed by the mitotic cyclin destruction machinery in *S. cerevisiae*. Curr Biol 8, 497–507.

Chen Y, Baker RE, Keith KC, Harris K, Stoler S, Fitzgerald-Hayes M (2000). The N terminus of the centromere H3-like protein Cse4p performs an essential function distinct from that of the histone fold domain. Mol Cell Biol 20, 7037–7048.

Choy JS, Acuna R, Au WC, Basrai MA (2011). A role for histone H4K16 hypoacetylation in *Saccharomyces cerevisiae* kinetochore function. Genetics 189, 11–21.

Choy JS, Mishra PK, Au WC, Basrai MA (2012). Insights into assembly and regulation of centromeric chromatin in *Saccharomyces cerevisiae*. Biochim Biophys Acta 1819, 776–783.

Clarke L, Carbon J (1980). Isolation of a yeast centromere and construction of functional small circular chromosomes. Nature 287, 504–509.

Cohen-Fix O, Koshland D (1999). Pds1p of budding yeast has dual roles: inhibition of anaphase initiation and regulation of mitotic exit. Genes Dev 13, 1950–1959.

Cohen-Fix O, Peters JM, Kirschner MW, Koshland D (1996). Anaphase initiation in *Saccharomyces cerevisiae* is controlled by the APC-dependent degradation of the anaphase inhibitor Pds1p. Genes Dev 10, 3081–3093.

Davies H, Hunter C, Smith R, Stephens P, Greenman C, Bignell G, Teague J, Butler A, Edkins S, Stevens C, *et al.* (2005). Somatic mutations of the protein kinase gene family in human lung cancer. Cancer Res 65, 7591–7595.

Degenhardt Y, Lampkin T (2010). Targeting Polo-like kinase in cancer therapy. Clin Cancer Res 16, 384–389.

Eckert CA, Gravdahl DJ, Megee PC (2007). The enhancement of pericentromeric cohesin association by conserved kinetochore components promotes high-fidelity chromosome segregation and is sensitive to microtubule-based tension. Genes Dev 21, 278–291.

Eng T, Guacci V, Koshland D (2014). ROCC, a conserved region in cohesin's Mcd1 subunit, is essential for the proper regulation of the maintenance of cohesion and establishment of condensation. Mol Biol Cell 25, 2351–2364.

Eng T, Guacci V, Koshland D (2015). Interallelic complementation provides functional evidence for cohesin-cohesin interactions on DNA. Mol Biol Cell 26, 4224–4235.

Gandhi R, Gillespie PJ, Hirano T (2006). Human Wapl is a cohesin-binding protein that promotes sister-chromatid resolution in mitotic prophase. Curr Biol 16, 2406–2417.

Gerton J (2005). Chromosome cohesion: a cycle of holding together and falling apart. PLoS Biol 3, e94.

Gerton JL (2007). Enhancing togetherness: kinetochores and cohesion. Genes Dev 21, 238–241.

Glynn EF, Megee PC, Yu HG, Mistrot C, Unal E, Koshland DE, DeRisi JL, Gerton JL (2004). Genome-wide mapping of the cohesin complex in the yeast *Saccharomyces cerevisiae*. PLoS Biol 2, E259.

Guacci V, Koshland D, Strunnikov A (1997). A direct link between sister chromatid cohesion and chromosome condensation revealed through the analysis of MCD1 in *S. cerevisiae*. Cell 91, 47–57.

Guacci V, Stricklin J, Bloom MS, Guo X, Bhatter M, Koshland D (2015). A novel mechanism for the establishment of sister chromatid cohesion by the ECO1 acetyltransferase. Mol Biol Cell 26, 117–133.

Haarhuis JH, Elbatsh AM, van den Broek B, Camps D, Erkan H, Jalink K, Medema RH, Rowland BD (2013). WAPL-mediated removal of cohesin protects against segregation errors and aneuploidy. Curr Biol 23, 2071–2077.

Haase J, Mishra PK, Stephens A, Haggerty R, Quammen C, Taylor RM 2nd, Yeh E, Basrai MA, Bloom K (2013). A 3D map of the yeast kinetochore reveals the presence of core and accessory centromere-specific histone. Curr Biol 23, 1939–1944.

Hardy CF, Pautz A (1996). A novel role for Cdc5p in DNA replication. Mol Cell Biol 16, 6775–6782.

Hartman T, Stead K, Koshland D, Guacci V (2000). Pds5p is an essential chromosomal protein required for both sister chromatid cohesion and condensation in *Saccharomyces cerevisiae*. J Cell Biol 151, 613–626.

Hauf S, Waizenegger IC, Peters JM (2001). Cohesin cleavage by separase required for anaphase and cytokinesis in human cells. Science 293, 1320–1323.

Ho Y, Gruhler A, Heilbut A, Bader GD, Moore L, Adams SL, Millar A, Taylor P, Bennett K, Boutilier K, *et al.* (2002). Systematic identification of protein complexes in Saccharomyces cerevisiae by mass spectrometry. Nature 415, 180–183.

Hornig NC, Uhlmann F (2004). Preferential cleavage of chromatin-bound cohesin after targeted phosphorylation by Polo-like kinase. EMBO J 23, 3144–3153.

Hu B, Itoh T, Mishra A, Katoh Y, Chan KL, Upcher W, Godlee C, Roig MB, Shirahige K, Nasmyth K (2011). ATP hydrolysis is required for relocating cohesin from sites occupied by its Scc2/4 loading complex. Curr Biol 21, 12–24.

Kan Z, Jaiswal BS, Stinson J, Janakiraman V, Bhatt D, Stern HM, Yue P, Haverty PM, Bourgon R, Zheng J, *et al.* (2010). Diverse somatic mutation patterns and pathway alterations in human cancers. Nature 466, 869–873.

Kastenmayer JP, Lee MS, Hong AL, Spencer FA, Basrai MA (2005). The C-terminal half of *Saccharomyces cerevisiae* Mad1p mediates spindle checkpoint function, chromosome transmission fidelity and CEN association. Genetics 170, 509–517.

Katis VL, Lipp JJ, Imre R, Bogdanova A, Okaz E, Habermann B, Mechtler K, Nasmyth K, Zachariae W (2010). Rec8 phosphorylation by casein kinase

1 and Cdc7-Dbf4 kinase regulates cohesin cleavage by separase during meiosis. Dev Cell 18, 397–409.
Kishi K, van Vugt MA, Okamoto K, Hayashi Y, Yaffe MB (2009). Functional dynamics of Polo-like kinase 1 at the centrosome. Mol Cell Biol 29, 3134–3150.
Kueng S, Hegemann B, Peters BH, Lipp JJ, Schleiffer A, Mechtler K, Peters JM (2006). Wapl controls the dynamic association of cohesin with chromatin. Cell 127, 955–967.
Laloraya S, Guacci V, Koshland D (2000). Chromosomal addresses of the cohesin component Mcd1p. J Cell Biol 151, 1047–1056.
Lee KS, Park JE, Asano S, Park CJ (2005). Yeast polo-like kinases: functionally conserved multitask mitotic regulators. Oncogene 24, 217–229.
Lengauer C, Kinzler KW, Vogelstein B (1998). Genetic instabilities in human cancers. Nature 396, 643–649.
Liang F, Jin F, Liu H, Wang Y (2009). The molecular function of the yeast polo-like kinase Cdc5 in Cdc14 release during early anaphase. Mol Biol Cell 20, 3671–3679.
Livak KJ, Schmittgen TD (2001). Analysis of relative gene expression data using real-time quantitative PCR and the 2(-Delta Delta C(T)) method. Methods 25, 402–408.
Ma L, Ho K, Piggott N, Luo Z, Measday V (2012). Interactions between the kinetochore complex and the protein kinase A pathway in *Saccharomyces cerevisiae*. G3 (Bethesda) 2, 831–841.
Maddox PS, Bloom KS, Salmon ED (2000). The polarity and dynamics of microtubule assembly in the budding yeast *Saccharomyces cerevisiae*. Nat Cell Biol 2, 36–41.
Maddox PS, Corbett KD, Desai A (2012). Structure, assembly and reading of centromeric chromatin. Curr Opin Genet Dev 22, 139–147.
Marston AL (2014). Chromosome segregation in budding yeast: sister chromatid cohesion and related mechanisms. Genetics 196, 31–63.
McKinley KL, Cheeseman IM (2014). Polo-like kinase 1 licenses CENP-A deposition at centromeres. Cell 158, 397–411.
Megee PC, Mistrot C, Guacci V, Koshland D (1999). The centromeric sister chromatid cohesion site directs Mcd1p binding to adjacent sequences. Mol Cell 4, 445–450.
Mishra PK, Au WC, Choy JS, Kuich PH, Baker RE, Foltz DR, Basrai MA (2011). Misregulation of Scm3p/HJURP causes chromosome instability in *Saccharomyces cerevisiae* and human cells. PLoS Genet 7, e1002303.
Mishra PK, Baum M, Carbon J (2007). Centromere size and position in *Candida albicans* are evolutionarily conserved independent of DNA sequence heterogeneity. Mol Genet Genomics 278, 455–465.
Mishra PK, Guo J, Dittman LE, Haase J, Yeh E, Bloom K, Basrai MA (2015). Pat1 protects centromere-specific histone H3 variant Cse4 from Psh1-mediated ubiquitination. Mol Biol Cell 26, 2067–2079.
Mishra PK, Ottmann AR, Basrai MA (2013). Structural integrity of centromeric chromatin and faithful chromosome segregation requires Pat1. Genetics 195, 369–379.
Nasmyth K (2002). Segregating sister genomes: the molecular biology of chromosome separation. Science 297, 559–565.
Newlon CS (1988). Yeast chromosome replication and segregation. Microbiol Rev 52, 568–601.
Ng TM, Waples WG, Lavoie BD, Biggins S (2009). Pericentromeric sister chromatid cohesion promotes kinetochore biorientation. Mol Biol Cell 20, 3818–3827.
Noble D, Kenna MA, Dix M, Skibbens RV, Unal E, Guacci V (2006). Intersection between the regulators of sister chromatid cohesion establishment and maintenance in budding yeast indicates a multi-step mechanism. Cell Cycle 5, 2528–2536.
Park CJ, Park JE, Karpova TS, Soung NK, Yu LR, Song S, Lee KH, Xia X, Kang E, Dabanoglu I, *et al.* (2008). Requirement for the budding yeast polo kinase Cdc5 in proper microtubule growth and dynamics. Eukaryotic Cell 7, 444–453.
Ratsima H, Ladouceur AM, Pascariu M, Sauve V, Salloum Z, Maddox PS, D'Amours D (2011). Independent modulation of the kinase and polo-box activities of Cdc5 protein unravels unique roles in the maintenance of genome stability. Proc Natl Acad Sci USA 108, E914–E923.
Richmond D, Rizkallah R, Liang F, Hurt MM, Wang Y (2013). Slk19 clusters kinetochores and facilitates chromosome bipolar attachment. Mol Biol Cell 24, 566–577.
Roccuzzo M, Visintin C, Tili F, Visintin R (2015). FEAR-mediated activation of Cdc14 is the limiting step for spindle elongation and anaphase progression. Nat Cell Biol 17, 251–261.
Rossio V, Galati E, Ferrari M, Pellicioli A, Sutani T, Shirahige K, Lucchini G, Piatti S (2010). The RSC chromatin-remodeling complex influences mitotic exit and adaptation to the spindle assembly checkpoint by controlling the Cdc14 phosphatase. J Cell Biol 191, 981–997.
Salmon ED, Shaw SL, Waters JC, Waterman-Storer CM, Maddox PS, Yeh E, Bloom K (2013). A high-resolution multimode digital microscope system. Methods Cell Biol 114, 179–210.
Santaguida S, Amon A (2015). Short- and long-term effects of chromosome mis-segregation and aneuploidy. Nat Rev Mol Cell Biol 16, 473–485.
Saunders MJ, Yeh E, Grunstein M, Bloom K (1990). Nucleosome depletion alters the chromatin structure of *Saccharomyces cerevisiae* centromeres. Mol Cell Biol 10, 5721–5727.
Sikorski RS, Hieter P (1989). A system of shuttle vectors and yeast host strains designed for efficient manipulation of DNA in Saccharomyces cerevisiae. Genetics 122, 19–27.
Singh VP, Gerton JL (2015). Cohesin and human disease: lessons from mouse models. Curr Opin Cell Biol 37, 9–17.
Skibbens RV, Marzillier J, Eastman L (2010). Cohesins coordinate gene transcriptions of related function within *Saccharomyces cerevisiae*. Cell Cycle 9, 1601–1606.
Snead JL, Sullivan M, Lowery DM, Cohen MS, Zhang C, Randle DH, Taunton J, Yaffe MB, Morgan DO, Shokat KM (2007). A coupled chemical-genetic and bioinformatic approach to Polo-like kinase pathway exploration. Chem Biol 14, 1261–1272.
Spencer F, Gerring SL, Connelly C, Hieter P (1990). Mitotic chromosome transmission fidelity mutants in *Saccharomyces cerevisiae*. Genetics 124, 237–249.
Stegmeier F, Visintin R, Amon A (2002). Separase, polo kinase, the kinetochore protein Slk19, and Spo12 function in a network that controls Cdc14 localization during early anaphase. Cell 108, 207–220.
Stephens P, Edkins S, Davies H, Greenman C, Cox C, Hunter C, Bignell G, Teague J, Smith R, Stevens C, *et al.* (2005). A screen of the complete protein kinase gene family identifies diverse patterns of somatic mutations in human breast cancer. Nat Genet 37, 590–592.
St-Pierre J, Douziech M, Bazile F, Pascariu M, Bonneil E, Sauve V, Ratsima H, D'Amours D (2009). Polo kinase regulates mitotic chromosome condensation by hyperactivation of condensin DNA supercoiling activity. Mol Cell 34, 416–426.
Surana U, Amon A, Dowzer C, McGrew J, Byers B, Nasmyth K (1993). Destruction of the CDC28/CLB mitotic kinase is not required for the metaphase to anaphase transition in budding yeast. EMBO J 12, 1969–1978.
Tanaka T, Cosma MP, Wirth K, Nasmyth K (1999). Identification of cohesin association sites at centromeres and along chromosome arms. Cell 98, 847–858.
Tong K, Skibbens RV (2014). Cohesin without cohesion: a novel role for Pds5 in *Saccharomyces cerevisiae*. PLoS One 9, e100470.
Uhlmann F, Lottspeich F, Nasmyth K (1999). Sister-chromatid separation at anaphase onset is promoted by cleavage of the cohesin subunit Scc1. Nature 400, 37–42.
Uhlmann F, Wernic D, Poupart MA, Koonin EV, Nasmyth K (2000). Cleavage of cohesin by the CD clan protease separin triggers anaphase in yeast. Cell 103, 375–386.
Verdaasdonk JS, Bloom K (2011). Centromeres: unique chromatin structures that drive chromosome segregation. Nat Rev Mol Cell Biol 12, 320–332.
Verdaasdonk JS, Gardner R, Stephens AD, Yeh E, Bloom K (2012). Tension-dependent nucleosome remodeling at the pericentromere in yeast. Mol Biol Cell 23, 2560–2570.
Waizenegger IC, Hauf S, Meinke A, Peters JM (2000). Two distinct pathways remove mammalian cohesin from chromosome arms in prophase and from centromeres in anaphase. Cell 103, 399–410.
Walters AD, May CK, Dauster ES, Cinquin BP, Smith EA, Robellet X, D'Amours D, Larabell CA, Cohen-Fix O (2014). The yeast polo kinase Cdc5 regulates the shape of the mitotic nucleus. Curr Biol 24, 2861–2867.
Weber SA, Gerton JL, Polancic JE, DeRisi JL, Koshland D, Megee PC (2004). The kinetochore is an enhancer of pericentric cohesin binding. PLoS Biol 2, E260.
Yeh E, Haase J, Paliulis LV, Joglekar A, Bond L, Bouck D, Salmon ED, Bloom KS (2008). Pericentric chromatin is organized into an intramolecular loop in mitosis. Curr Biol 18, 81–90.
Zitouni S, Nabais C, Jana SC, Guerrero A, Bettencourt-Dias M (2014). Polo-like kinases: structural variations lead to multiple functions. Nat Rev Mol Cell Biol 15, 433–452.